Exploring the Role of Bromine at C(10) of (+)-4-[2-[4-(8-Chloro-3,10-dibromo-6,11-dihydro-5H-benzo[5,6]cyclohepta[1,2-b]pyridin-11(*R*)-yl)-1-piperidinyl]-2-oxoethyl]-1-piperidinecarboxamide (Sch-66336): The Discovery of Indolocycloheptapyridine Inhibitors of Farnesyl Protein Transferase

Arthur G. Taveras,* Cynthia Aki, Jianping Chao, Ronald J. Doll, Tarik Lalwani, Viyyoor Girijavallabhan, Corey L. Strickland, William T. Windsor, Patricia Weber, Frank Hollinger, Mark Snow, Robert Patton, Paul Kirschmeier, Linda James, Ming Liu, and Amin Nomeir

Departments of Chemistry and Tumor Biology, Schering-Plough Research Institute, 2015 Galloping Hill Road, Kenilworth, New Jersey 07033

Received October 8, 2001

The 10-bromobenzocycloheptapyridyl farnesyl transferase inhibitor (FTI) Sch-66336 (**1**) is currently under clinical evaluation for the treatment of human cancers. During structure−activity relationship development leading to **1**, 10-bromobenzocycloheptapyridyl FTIs were found to be more potent than analogous compounds lacking the 10-Br substituent. This potency enhancement was believed to be due, in part, to an increase in conformational rigidity as the 10-bromo substituent could restrict the conformation of the appended C(11) piperidyl substituent in an axial orientation. A novel and potent class of FTIs, represented by indolocycloheptapyridine Sch-207758 [(+)-**10a**], have been designed based on this principle. Although structural and thermodynamic results suggest that entropy plays a crucial role in the increased potency observed with (+)-**10a** through conformational constraints and solvation effects, the results also indicate that the indolocycloheptapyridine moiety in (+)-**10a** provides increased hydrophobic interactions with the protein through the addition of the indole group. This report details the X-ray structure and the thermodynamic and pharmacokinetic profiles of (+)-**10a**, as well as the synthesis of indolocycloheptapyridine FTIs and their potencies in biochemical and biological assays.

Introduction

Understanding the genetic basis of human diseases such as cancer may lead to novel therapeutic approaches to treat these illnesses. Many human cancers of the bladder, lung, colon, and pancreas have been associated with an oncogenic *ras*, and its discovery has triggered extensive studies aimed at understanding more fully its role in the mechanisms leading to tumorigenicity.[1] What has emerged is that the farnesylation of Ras, the protein product encoded by *ras*, is required for downstream signaling of cell growth and proliferation in both normal and tumor cells.[2a] Apart from Ras, other proteins including RhoB, CENP-E, and CENP-F are also farnesylated and are also involved in mediating cell growth.[2b−f] Inhibition of the enzyme that catalyzes the farnesylation of Ras, farnesyl protein transferase (FPT), leads to inhibition of tumor cell growth in vitro and in vivo.[3] X-ray crystal structure analysis in conjunction with biological studies have delineated the catalytic site of FPT-mediated Ras farnesylation.[4] The association of a trimeric complex consisting of FPT, the activated farnesylating agent farnesyl pyrophosphate (FPP), and a four amino acid portion of the Ras protein (commonly described as the CaaX motif) triggers Ras farnesylation.[5] The transfer of a farnesyl group from FPP to a cysteine residue of the CaaX motif of Ras leads to a farnesylated protein, which, following additional modification, actively participates in signal transduction leading to cellular proliferation. Inhibition of this catalytic event might, therefore, be a novel approach for the treatment of cancers.

Chart 1

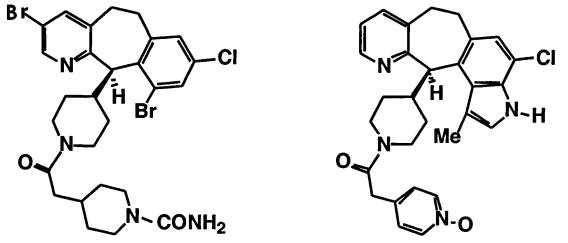

Sch-66336 (1) **Sch-207758 [(+) 10a]**

Several farnesyl transferase inhibitors (FTIs) have been identified, which antagonize the binding of the prenylating agent FPP and which antagonize the association of the CaaX motif of Ras with FPT.[6] Among these, benzocycloheptapyridines have been shown to compete with the binding of Ras to FPT, to inhibit the farnesylation of Ras in vitro and to inhibit tumor growth in vivo in orally treated mice.[7] Sch-66336 (**1**) (Chart 1), a potent and orally efficacious 3,10-dibromobenzocycloheptapyridine FTI, has been progressed to a Phase II clinical evaluation of its potential as a therapeutic agent for the treatment of human cancers.[8]

Details of the structure−activity relationship (SAR) studies leading to the discovery of **1** have recently been

* To whom correspondence should be addressed. Tel: (908)740-3130. Fax: (908)740-7152. E-mail: arthur.taveras@spcorp.com.

10.1021/jm010463v CCC: $22.00
Published on Web 08/06/2002

Scheme 1

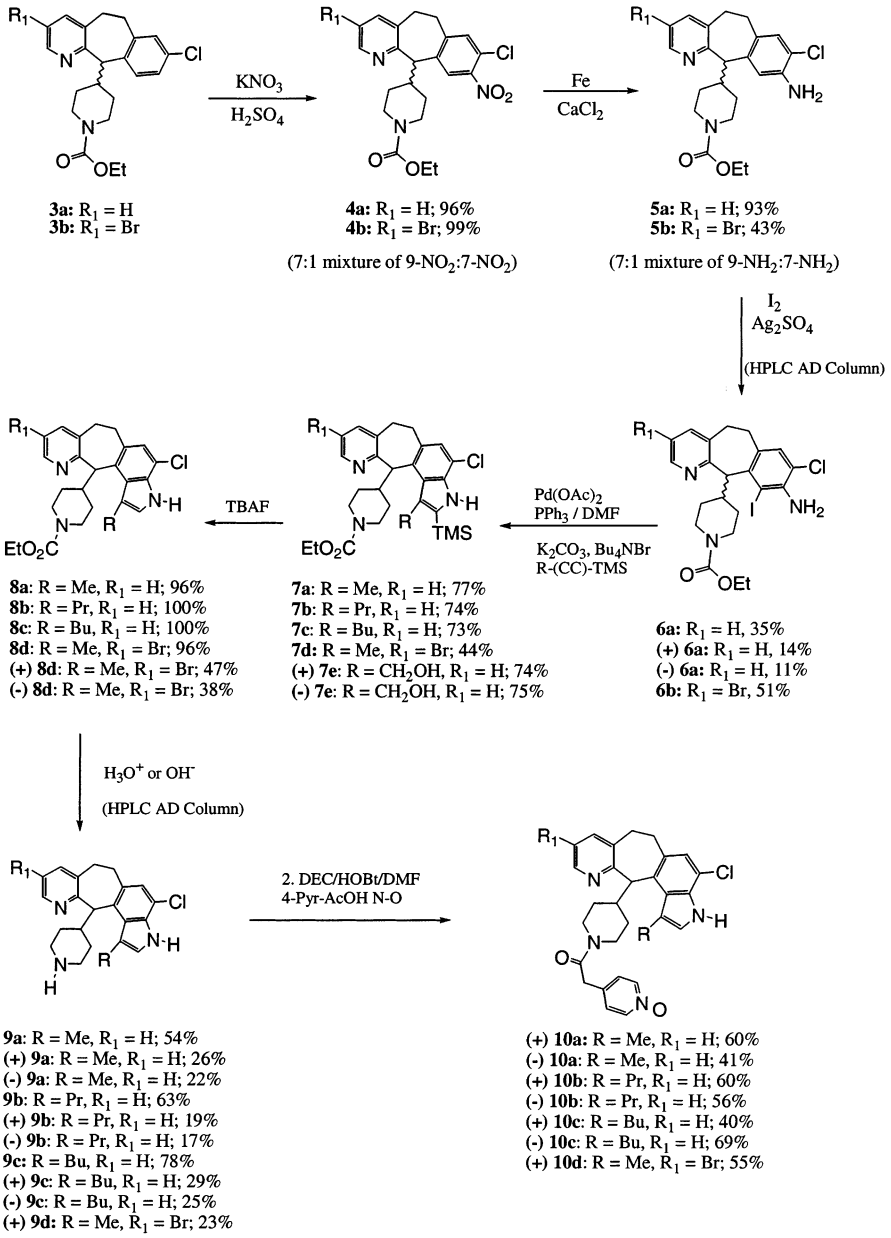

3a: R_1 = H
3b: R_1 = Br

4a: R_1 = H; 96%
4b: R_1 = Br; 99%
(7:1 mixture of 9-NO_2:7-NO_2)

5a: R_1 = H; 93%
5b: R_1 = Br; 43%
(7:1 mixture of 9-NH_2:7-NH_2)

6a: R_1 = H, 35%
(+) 6a: R_1 = H, 14%
(-) 6a: R_1 = H, 11%
6b: R_1 = Br, 51%

7a: R = Me, R_1 = H; 77%
7b: R = Pr, R_1 = H; 74%
7c: R = Bu, R_1 = H; 73%
7d: R = Me, R_1 = Br; 44%
(+) 7e: R = CH_2OH, R_1 = H; 74%
(-) 7e: R = CH_2OH, R_1 = H; 75%

8a: R = Me, R_1 = H; 96%
8b: R = Pr, R_1 = H; 100%
8c: R = Bu, R_1 = H; 100%
8d: R = Me, R_1 = Br; 96%
(+) 8d: R = Me, R_1 = Br; 47%
(-) 8d: R = Me, R_1 = Br; 38%

9a: R = Me, R_1 = H; 54%
(+) 9a: R = Me, R_1 = H; 26%
(-) 9a: R = Me, R_1 = H; 22%
9b: R = Pr, R_1 = H; 63%
(+) 9b: R = Pr, R_1 = H; 19%
(-) 9b: R = Pr, R_1 = H; 17%
9c: R = Bu, R_1 = H; 78%
(+) 9c: R = Bu, R_1 = H; 29%
(-) 9c: R = Bu, R_1 = H; 25%
(+) 9d: R = Me, R_1 = Br; 23%

(+) 10a: R = Me, R_1 = H; 60%
(-) 10a: R = Me, R_1 = H; 41%
(+) 10b: R = Pr, R_1 = H; 60%
(-) 10b: R = Pr, R_1 = H; 56%
(+) 10c: R = Bu, R_1 = H; 40%
(-) 10c: R = Bu, R_1 = H; 69%
(+) 10d: R = Me, R_1 = Br; 55%

published.[8a] Our SAR studies of benzocycloheptapyridine FTIs have revealed a marked improvement in FPT binding affinity for compounds substituted at the C(10) position of the tricyclic moiety. Accordingly, the C(10) des bromo analogue of **1** inhibits FPT-mediated Ras farnesylation with an IC_{50} = 19 nM, while the IC_{50} of **1** itself is 1.9 nM. This 10-fold improvement in FPT potency has also been translated to other members of this tricyclic series of FTIs upon C(10) bromination. The mechanism by which the C(10) bromine substituent contributed to the observed potency enhancement of benzocycloheptapyridine FTIs was not readily apparent.

The X-ray crystal structure of the FPT:**1** complex has been determined and provides the first insight into the binding orientation of benzocycloheptapyridine FTIs.[9] It can be seen that much of **1** interacts with the β-subunit of FPT while the tricyclic moiety spans both the α- and the β-subunits of FPT. A π,π-aromatic interaction between the phenyl ring of the tricycle and a tryptophan-102β residue of FPT is observed in the X-ray crystal structure of the FPT:**1** complex. The C(10) bromine substituent of **1** is located near lipophilic residues and hydrophobic/van der Waals interactions contribute to the potency enhancement seen with 3,10-dibromobenzocycloheptapyridine FTIs. In addition, the 10-bromo substituent in **1** sterically interfered, we believed, with the neighboring C(11) piperidyl substituent thereby helping to orient this appendage in the axial conformation seen in the X-ray crystal structure of the complex.

We engaged in a FPT inhibitor design program with the goal of discovering novel FTIs that would mimic the hypothesized role of the C(10) substituent in 10-bromobenzocycloheptapyridine FTIs as a support scaffold stabilizing a specific orientation of the C(11) piperidyl substituent. Accordingly, we prepared novel tetracyclic derivatives of **1**, represented by indolocycloheptapyridine (+)-**10a**, and found these compounds to be potent inhibitors of FPT. Herein, we report the design, synthesis, and biological evaluation of several indolocyclo-

Scheme 2

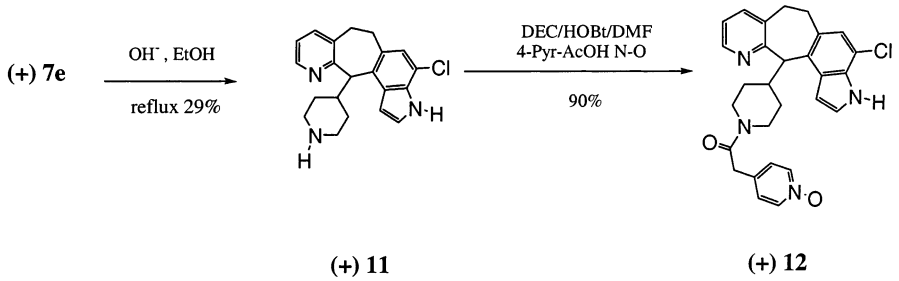

(+) 11 (+) 12

Scheme 3

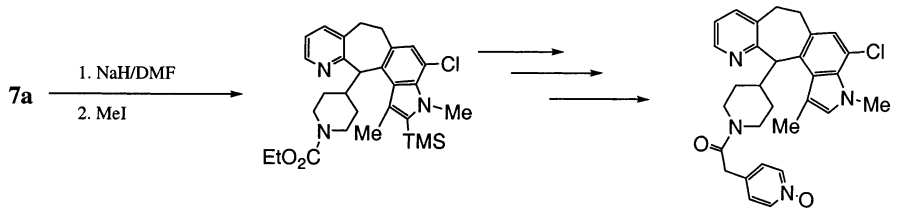

13 14

heptapyridines. The pharmacokinetic profile of (+)-**10a**, the thermodynamics of binding, and an X-ray crystal structure determination of the r-FPT:(+)-**10a** complex will also be discussed.

Chemistry

The general sequence utilized to prepare C(11) piperidine-substituted indolocycloheptapyridines (i.e., (+)-**10a**) featured an intermolecular Heck reaction between iodoanilines **6a**,**b** and substituted trimethylsilylalkylacetylenes. Subsequent transformations of the silylated indole products **7a**−**e** afforded the desired β-substituted indole targets **10a**−**d**, **12**, **14**, and **21**.

Iodoanilines **6a**,**b** were prepared in three steps from piperidines **3a**,**b**.[10] Electrophilic aromatic nitration of carbamates **3a**,**b** afforded regioisomeric mixtures of 9- and 7-nitro compounds **4a**,**b**. Iron-assisted reduction of nitrobenzenes **4a**,**b** gave anilines **5a**,**b**, which delivered chloroiodoanilines **6a**,**b** upon treatment with iodine and silver sulfate in 85% ethanol (Scheme 1).

Palladium-catalyzed Heck reaction of **6a**,**b** with trimethylsilylpropyne, -pentyne, or -hexyne afforded trimethylsilyl pyrroles **7a**−**d**. Desilylation using tetrabutylammonium fluoride afforded pyrroles **8a**−**d** in excellent yields. Aqueous acid hydrolysis of the carbamate function in **8a**−**d** provided piperidine amines **9a**−**d**, which were resolved by high-performance liquid chromatography (HPLC) (ChiralPak AD column, hexane-2-propanol). Coupling of the resolved enantiomers with pyridylacetic acid N-oxide using DEC and HOBt yielded amides **10a**−**d**.

An intermolecular Heck reaction of iodoaniline (+)-**6a** with trimethylsilylhydroxypropyne at 85 °C provided hydroxymethylindole (+)-**7e** as illustrated in Scheme 1. Ethanolic hydroxide-mediated saponification of the carbamate function in (+)-**7e** (Scheme 2) generated deshydroxymethyl indole (+)-**11**. Conversion of (+)-**11** to pyridylacetamide N-oxide (+)-**12** proceeded in excellent yield.

Alkylation of the sodium pyrrolide of **7a** with methyl iodide afforded N-methylindole **13**, which was similarly transformed to pyridyl N-oxide **14** as described earlier (Scheme 3).

3-Bromoindolocycloheptapyridine **21** was prepared as illustrated in Scheme 4 from iodoaniline **17** following electrophilic aromatic iodination of **16** with iodine and silver sulfate.[11] The intermolecular Heck reaction of **17** with trimethylsilylpropyne was most efficiently effected at 74 °C; higher temperatures resulted in additional side reactions. This transformation proceeded slowly as compared to that seen with **6b**. Presumably, the increased congestion near the aryl iodide reaction center imparted by the sp^2-hybridized C(11) piperidine appendage as compared to a more exposed iodoaniline for the C(11) sp^3-hybridized center in **6b** accounts for the decreased rate of reaction for **17**. Indole **18** was desilylated using TBAF while aqueous acid hydrolysis of the resulting carbamate **19** afforded piperidine **20**. Pyridyl N-oxide **21** was subsequently prepared by treatment of **20** with 4-pyridylacetic acid N-oxide, DEC, and HOBt in dimethylformamide (DMF). Neither **21** nor **20** could be separated into their individual atropisomers by chiral HPLC (AD column).[12]

Indole **20**, shown in Scheme 4, could not be used to prepare pyridyl N-oxide **10d**. Whereas 10-bromobenzocycloheptapyridines[8a] readily undergo olefin reduction with DIBAL, the olefin in **20** was stable in refluxing toluene with up to 10 equiv of DIBAL. Compound (+)-**10d** was instead prepared from **6b** as illustrated in Scheme 1.

Biological Methods

The FPT activity of the compounds listed in Table 1 was determined by measuring the transfer of [^{3}H]-farnesyl from [^{3}H]FPP to trichloroacetic acid precipitable His^6-H-Ras-CVLS. Experimental details of the FPT assay used in our study have been previously recorded by Bishop et al.[7a] The effect of compounds on Ras processing in Cos-1 monkey kidney cells transiently expressing either H-Ras-val^{12}-CVLS or H-Ras-val^{12} was performed according to the protocol disclosed previously.[7a]

Scheme 4

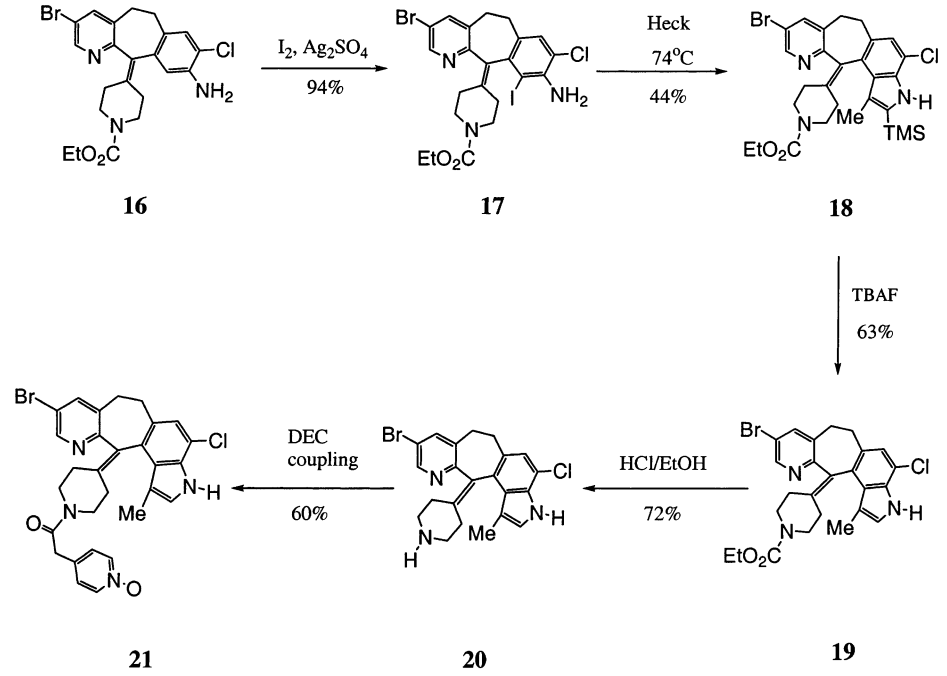

Table 1. FPT Inhibitory Potencies of Indolo- and Benzocycloheptapyridines

entry	Hras FPT IC_{50} (nM)[a]	entry	Hras FPT IC_{50} (nM)[a]
(+)-**10a**	7.4 ± 0.9	(−)-**10a**	28 ± 3.8
(+)-**10b**	65 ± 2.5	(−)-**10b**	>190
(+)-**10c**	69 ± 1	(−)-**10c**	>180
(+)-**10d**	2.6 ± 1	(+)-**12**	42 ± 1
(+)-**14**	>190	(±)-**21**	5.8 ± 2.5
(+)-**22a**[c]	34 ± 3	(+)-**22b**[d]	19 ± 1.1
(+)-**22c**[e]	2.0 ± 0.5	**1**	1.9 ± 0.1

[a] Data shown are the mean of two experiments. A standard FTI (related to the compounds described) was run with each set of compounds. The range of IC_{50} values for this compound was 0.8−2.2 nM over 33 separate determinations on different days. The mean IC_{50} for this compound was 1.5 ± 0.4 nM (mean ± standard deviation). The coefficient of variation for the assay (comparing no inhibitor control values) was typically on the order of 6.8%. [b] Single point determinations. [c] See ref 10. [d] See ref 8a. [e] See ref 13.

Results and Discussion

During the discovery of **1** and other benzocycloheptapyridine FTIs, we had observed a significant potency enhancement in both enzyme and cellular assays for 10-bromobenzocycloheptapyridine FTIs as compared to their 10-des-bromo derivatives.[8a] Accordingly, 10-des-bromo **22a** (Chart 2) demonstrated FPT and Cos cell IC_{50} values of 34 and 560 nM, respectively, while the corresponding 10-bromo analogue **22c** inhibited Ras farnesylation in these assays at concentrations of 2.0 and 10 nM (IC_{50} values), respectively (Table 1).[8a]

Other differences, particularly in chemical reactivity and in thermal stability, between 10-bromo and 10-des-bromo analogues were also noted. 10-Bromobenzocycloheptapyridine **23b**, having a piperidyl moiety attached to the C(11) atom by an olefin unit, exists in two atropisomeric forms, and these atropisomers can be separated by HPLC (ChiralPak AD) into enantiomers (+)-**23b** and (−)-**23b**.[12] 10-Des-bromobenzocycloheptapyridines (+)-**23a** and (−)-**23a** readily interconvert at room temperature and cannot be isolated as individual enantiomers (eq 1).[12]

Chart 2

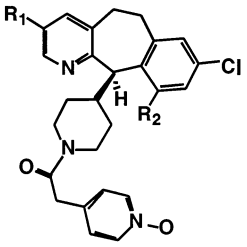

22a: R_1 = Br, R_2 = H;
22b: R_1 = H, R_2 = Br;
22c: R_1 = Br, R_2 = Br.

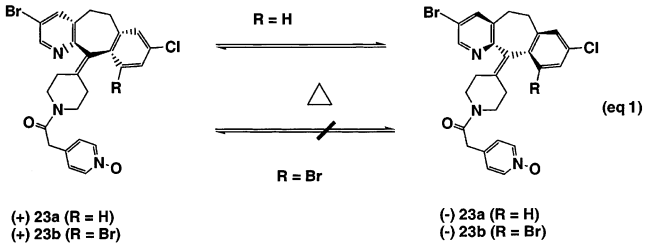

These observations point to a specific role of the C(10) bromine substituent in benzocycloheptapyridine FTIs. We propose that the aforementioned effects are related, in part, to an intramolecular steric interaction between the C(10) bromine atom and the C(11) piperidyl moiety. The bromine substituent at C(10) may encourage the C(11) piperidyl moiety to adopt a conformation that would alleviate steric interactions between these two bulky substituents (eq 2). Such conformational constraints would translate into a decrease in entropy resulting in improved binding affinity of 10-bromine-containing FTIs. This conformational rigidity exerted by the C(10) bromine atom would also prevent interconversion of atropisomeric 10-bromobenzocycloheptapyridine FTIs (i.e., **23b**).

The X-ray crystal structure of **1** complexed with FPT provided the first insight into the binding orientation

(and presumably bioactive conformation) of 8-chlorobenzocycloheptapyridine compounds in the active site of FPT.[9] In accordance with our proposal based on stereoelectronic considerations of the experimental observations, the C(11) piperidyl substituent was found by X-ray to be oriented in an axial or pseudoaxial conformation relative to the tricyclic moiety of **1**.

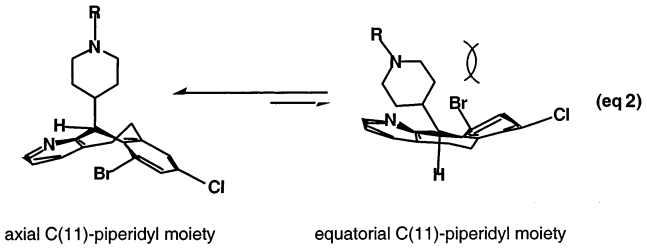

The idea that a bulky C(10) substituent could orient the C(11) piperidyl moiety of benzocycloheptapyridine FTIs in the bioactive, pseudoaxial conformation became the basis for our de novo design of the next generation of benzocycloheptapyridine FPT inhibitors. Key features of the molecular interaction between **1** and FPT critical to the design of novel FTIs were the orientation of the C(11) piperidyl substituent and the edge to face π,π-aromatic interaction that the phenyl ring of the tricycle made with the tryptophan-102β residue of FPT.[9] Indolocycloheptapyridines [i.e., (+)-**10a**, (+)-**10b**, (+)-**10c**, (+)-**10d**, and **21**] were designed as potential inhibitors of FPT whereby the substituted pyrrole ring attached to the tricyclic moiety could sterically orient the C(11) piperidyl moiety in an axial environment and interact favorably with the tryptophan-102 residue in the β-subunit of FPT. Accordingly, methyl indole (+)-**10a**, with an IC_{50} of 7.4 nM, is 3-fold more potent than the 10-bromo FTI analogue (+)-**22b** (IC_{50} = 19 nM) thereby confirming the favorable role of the methyl indole moiety. Furthermore, the enhanced potency of dihalo methyl indole (+)-**10d** (IC_{50} = 2.6 nM) was comparable to that of the trihalo compound **1** (IC_{50} = 1.9 nM).

X-ray Crystal Structure Analysis of r-FPT:(+)-10a. An X-ray crystal structure determination of the complex between rat FPT and indolocycloheptapyridine (+)-**10a** reveals the binding orientation of this novel indole FTI in the active site of rFPT (Figure 1). Indolocycloheptapyridine (+)-**10a** is seen to occupy the same binding site as **1**;[9] however, with (+)-**10a**, the indole N−H is seen to engage in a protio-π aromatic interaction with Trp102β of FPT. This interaction may contribute to the improved potency of indolocycloheptapyridines over analogous 10-bromobenzocycloheptapyridines (Table 1). Additional support for the importance of this protio-π aromatic interaction with (+)-**10a** is demonstrated by the decrease in activity of the indole N−CH_3 derivative (+)-**14** (IC_{50} > 190 nM). The N-methyl substituent in (+)-**14** may also sterically interfere with a neighboring Trp102β thereby affecting its binding interaction with FPT and reducing its overall potency.

The X-ray structure of the FPT:(+)-**10a** complex shows the β-methyl substituent on the indole ring of (+)-**10a** protruding toward the C(11) piperidyl moiety, orienting it in an axial conformation. This methyl substituent appears to buttress the axially oriented C(11) piperidyl substituent in accordance with our design strategy. The greater binding affinity of indolocycloheptapyridine (+)-**10a** as compared to its analogous 10-bromocycloheptapyridine[13] (**22b**) may be due, in part, to the increased conformational constraints imposed by the β-methyl substituent of the indole preventing the C(11) piperidyl moiety from extending into an equatorial conformation. This hypothesis is further supported by the 6-fold decrease in FPT potency (IC_{50} = 42 nM) of the des-methyl analogue (+)-**12** where a hydrogen atom would exert less steric constraints than would a methyl group. The increase in affinity for the methyl−indole moiety is also likely to arise from favorable hydrophobic interactions with serine 99.

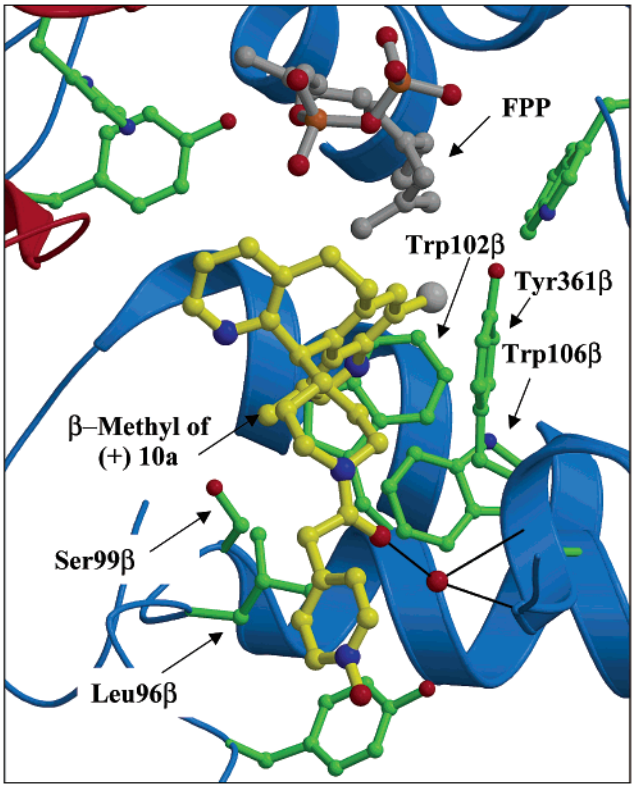

Figure 1. X-ray crystal structure of Sch-207758-r-FPT.

The extent to which the indole moiety may be substituted is limited by the spatial constraints exerted by the protein in this region. The β-methyl substituent on the indole moiety of (+)-**10a** is located in a fairly congested region of FPT whereby further substitution would be expected to result in decreased potency as a consequence of increased steric hindrance. Accordingly, propyl- and butyl-substituted indoles (+)-**10b** and (+)-**10c**, respectively, were found to be less potent (IC_{50} > 180 nM) than the smaller methyl-substituted analogue (+)-**10a**.

The opposite enantiomer of methyl indole (+)-**10a**, (−)-**10a**, was also fairly potent as an FTI having an IC_{50} of 28 nM. This result is interesting and unexpected since we have reported that 10-bromobenzocycloheptapyridines having C(11) *S* stereochemistry have never been found to be potent inhibitors of FPT.[8a] The reasons for the enhanced potency of (−)-**10a** are unclear but may be related to additional interactions made between the indole structure and the amino acid residues in the α-subunit of FPT.[14] An X-ray crystal structure of the r-FPT:(−)-**10a** complex could not be obtained to confirm this suggestion.

Thermodynamic Binding Analysis. Isothermal titration calorimetry measurements were performed to determine the thermodynamic contributions of (+)-**10a** binding to FPT. The free energy of binding (ΔG°_{bind}) was −10.3 (±0.1) kcal/mol (K_d = 28 nM). The corresponding enthalpic (ΔH°_{bind}) and entropic ($T\Delta S^\circ_{bind}$) values were −7.1 (±0.05) and +3 (±0.1) kcal/mol, respectively. Thermodynamic analysis of tricyclic inhibitors binding to FPT showed that the addition of the Br atoms to the tricyclic group enhanced the affinity of the compounds through an increase in van der Waals interactions.[9] For these compounds, 1 kcal/mol ΔH°_{bind} per each 20 Å^2 of buried nonpolar surface area from the halogen was obtained.

In our current study, the entropy value for (+)-**10a** ($T\Delta S^\circ_{bind}$ = +3 kcal/mol) is significantly more favorable than that observed previously in the 10-Br-substituted compounds ($T\Delta S^\circ_{bind}$ = −0.1 to −1.6 kcal/mol).[9] Some of the favorable entropic contributions for (+)-**10a** may come from the increased conformational constraint of the inhibitor imposed by the β-methyl indole substituent. Another favorable contribution to the entropy term may come from the displacement of water molecules upon inhibitor binding to protein. At least two water molecules are released upon (+)-**10a** binding. The first water molecule, which is also displaced by the 10-Br-containing compounds, interacts with Ser99β in the uncomplexed FPT. The second water molecule, which is unique to (+)-**10a**-like compounds containing the β-methyl indole, hydrogen bonds to the indole nitrogen of the inhibitor when it is free in solution. The X-ray structure indicates that the indole N−H is not hydrogen-bonded to a water molecule when bound to FPT; however, it does form an electrostatic protio-π aromatic interaction with Trp102β. The release of one additional water molecule as compared to a C(10) bromo compound is estimated to contribute up to +2 kcal/mol in favorable entropic energy.[16] It appears that the incorporation of the β-methylindole N−H substituent to the tricyclic inhibitors has the advantage of providing favorable entropic contributions toward protein binding through both conformational constraints and solvation effects. Replacement of aromatic rings involved in electrostatic protio-π aromatic interactions with an indole ring could be a general approach to improve the entropic contribution toward binding and increase the overall affinity of FTIs.

Cellular Evaluation of Indolocycloheptapyridine FTIs. The cellular activity of the more potent indolocycloheptapyridine FPT inhibitors listed in Table 1 was determined by examining the effect on Ras processing in Cos-1 monkey kidney cells transiently expressing either H-Ras-val^{12}-CVLS or H-Ras-val.^{12} The cellular potency of (+)-**10a** was found to be 250 nM (IC_{50}) in the cos cell assay. As had been seen with 3-bromobenzocycloheptapyridine FTIs (i.e., **22a** and **22c**),[7d,8a] introduction of a 3-bromo substituent onto methylindolocycloheptapyridines (i.e., (+)-**10a**) greatly enhanced the potency of the FTIs in both the enzyme and the cellular assays. Accordingly, 3-bromoindolocycloheptapyridines **21** and (+)-**10d** demonstrated cos cell potencies (IC_{50}) of 48 and 10 nM, respectively. The cellular activity for (+)-**10d** is equivalent to that of the 3,10-dibromo analogue **22c** (IC_{50} = 10 nM).

Pharmacokinetic Evaluation of (+)-10a. Indolocycloheptapyridine (+)-**10a** has been evaluated in a pharmacokinetic screen according to the procedures already reported.[8,15] Nude mice treated orally with 25 mpk of compound dissolved in aqueous HPβCD solution exhibited an AUC of 2.9 μM hr with a C_{max} of 2 μM. When this sample was dosed intravenously, an AUC of 34 μM hr and a C_{max} of 40 μM were sustained up to 7 h following treatment. The half-life of this compound could not be calculated since the concentration of (+)-**10a** in the serum appeared to increase over time in the oral study up to 4 h.

Conclusion

The combined chemical reactivity, X-ray crystal structure determination, and biological activity profile of 10-bromobenzocycloheptapyridine FTIs suggest, in part, a favorable conformational effect due to the 10-bromo substituent. Indolocycloheptapyridines (+)-**10a**−**d**, (+)-**12**, and **21** were designed to mimic the proposed role of the 10-bromosubstituent in 10-bromobenzocycloheptapyridine FTIs buttressing the C(11) piperidyl moiety in an axial conformation. Novel tetracyclic derivatives of **1**, represented by indolocycloheptapyridine (+)-**10a**, were prepared and found to potently inhibit Ras processing in enzyme and cellular assays and to do so more effectively than analogous 10-bromobenzocycloheptapyridine FTIs. The crystal structure and thermodynamic results suggest that favorable entropic contributions play a role in the increased potency through conformational constraints imposed by the indolocycloheptapyridine moiety of the compound and solvation effects. These discoveries demonstrate how critical analyses of chemical, biological, and structural results can initiate the design of novel enzyme inhibitors.

Experimental Section

General Methods. All reagents were used without further purification. Melting points were determined using an Electrothermal Digital Melting Point apparatus and are uncorrected. Elemental analyses were performed on either a Leeman CE 440 or a FISONS EA 1108 elemental analyzer. ^{1}H and ^{13}C nuclear magnetic resonance (NMR) spectra were recorded on either a Varian VXR-200 (200 MHz) or Varian Gemini-300 (300 MHz) NMR spectrometers using Me_4Si as an internal standard. For ^{13}C NMR, a Nalorac Quad nuclei probe was used. Fourier transform infrared (FT-IR) spectra were recorded using a BOMEN Michelson 120 spectrometer. Mass spectra were recorded using either EXTREL 401 (Chemical Ionization), JEOL, or MAT-90 (FAB), or VG ZAB-SE (SIMS) mass spectrometers. Microanalyses were performed by the Physical-Analytical Chemistry Department at Schering-Plough Research Institute.

X-ray Crystallography. Crystals of the FPT:(+)-**10a** complex were prepared by cocrystallizing (+)-**10a** with FPT using methods previously described.[9] X-ray diffraction data were collected on a Rigaku rotating anode generator equipped with MSC mirrors and a Raxis-IIc image plate detector. The data extend to 2.6 Å resolution and have a R_{merge} of 6.4% with a 3.5-fold multiplicity. The structure was refined using XPLOR98.1 (Molecular Simulations Inc.) to an R_{factor} of 21%.

Isothermal Titration Calorimetry. Heats of complex formation were measured by tritrating inhibitor into a Human FPT solution using an isothermal titration calorimeter (MCS, MicroCal Corp., Northhampton, MA). The sample cell contained 10 μM FPT in the presence of 16 μM farnesyl diphosphate (Sigma), and the inhibitor solution contained 100 μM inhibitor in the presence of 16 μM farnesyl diphosphate.

Binding studies were performed in 40 mM Hepes, 1 mM DTT, pH 7.4, at 20 °C. Protein purification and titration conditions are identical to those described by Strickland.[9]

(±)-4-(8-Chloro-6,11-dihydro-7/9-nitro-5*H*-benzo[5,6]-cyclohepta[1,2-b]pyridin-11-yl)-1-piperidinecarboxylic Acid Ethyl Ester (4a). Compound **4a** was prepared according to the procedures described in ref 8a. Data for **4a**: solid, 85 g, 96%. ^{1}H NMR (200 MHz, acetone-d_6, 7:1 mixture of regioismers of 9-nitro:7-nitro): δ 1.05−1.60 (m, 4H), 1.20 (overlapping t, 3H, J = 7 Hz), 2.50−3.30 (m, 5H), 3.53 (m, 2H), 3.92−4.25 (m, 3H), 4.03 (overlapping q, 2H, J = 7 Hz), 7.20 (dd, 1H, J = 4 Hz, J = 8 Hz), 7.49−7.64 (m, 1H), 7.56 (overlapping s, 1H), 7.95 (s, 1H), 8.35 (m, 1H). MS (CI): m/z 430 (MH^+, 100%). Anal. ($C_{22}H_{24}N_3O_4Cl\cdot0.3H_2O\cdot0.1C_6H_{14}$) C, H, N.

(±)-4-(3-Bromo-8-chloro-6,11-dihydro-7/9-nitro-5*H*-benzo[5,6]cyclohepta[1,2-b]pyridin-11-yl)-1-piperidinecarboxylic Acid Ethyl Ester (4b). Compound **4b** was prepared according to the procedures described in ref 8a. Data for **4b**: solid, 72.27 g, 99%. ^{1}H NMR (200 MHz, $CDCl_3$, mixture of regioismers of 9-nitro and 7-nitro): δ 0.85−1.95 (m, 4H), 1.25 (overlapping t, 3H, J = 7 Hz), 2.30 (m, 1H), 2.62 (m, 2H), 2.96 (m, 2H), 3.2−4.3 (m, 5H), 4.15 (overlapping q, 2H, J = 7 Hz), 7.36 (s, 1H), 7.59 (m, 1H), 7.75 (s, 1H), 8.45 (d, 1H, J = 1 Hz). MS (FAB): m/z 508 (MH^+, 75%), 510 ($MH^+ + 2$, 100%). HRFABMS calcd for $C_{22}H_{24}N_3O_4BrCl$, M_r 508.0639 (MH^+); found, 508.0621.

(±)-4-(8-Chloro-6,11-dihydro-7/9-amino-5*H*-benzo[5,6]-cyclohepta[1,2-b]pyridin-11-yl)-1-piperidinecarboxylic Acid Ethyl Ester (5a). Compound **5a** was prepared according to the procedures described in ref 8a. Data for **5a**: solid, 73.5 g, 93%. ^{1}H NMR (200 MHz, $CDCl_3$, 7:1 mixture of regioismers of 9-amino:7-amino): δ 1.06−1.60 (m, 4H), 1.20 (overlapping t, 3H, J = 7 Hz), 2.10−3.04 (m, 5H), 3.35 (m, 2H), 3.78 (d, 1H, J = 10 Hz), 3.90 (broad s, 1H), 3.95−4.21 (m, 2H), 4.03 (overlapping q, 2H, J = 7 Hz), 6.60 (s, 1H), 7.03 (s, 1H), 7.07 (dd, 1H, J = 4 Hz, J = 8 Hz), 7.39 (d, 1H, J = 8 Hz), 8.30 (dd, 1H, J = 1 Hz, J = 4 Hz). MS (CI): m/z 400 (MH^+, 100%). Anal. ($C_{22}H_{26}N_3O_2Cl\cdot1.4H_2O\cdot0.4C_6H_{14}$) C, H, N.

(±)-4-(3-Bromo-8-chloro-6,11-dihydro-9-amino-5*H*-benzo[5,6]cyclohepta[1,2-b]pyridin-11-yl)-1-piperidinecarboxylic Acid Ethyl Ester (5b). Compound **5b** was prepared according to the procedures described in ref 8a. Data for **5b**: solid, 29.4 g, 43%. ^{1}H NMR (200 MHz, $CDCl_3$): δ 1.05−1.72 (m, 4H), 1.26 (overlapping t, 3H, J = 7 Hz), 2.3 (m, 1H), 2.50−3.10 (m, 6H), 3.35 (m, 2H), 3.82 (d, 1H, J = 10 Hz), 4.00−4.32 (m, 2H), 4.13 (overlapping q, 2H, J = 7 Hz), 6.60 (s, 1H), 7.06 (s, 1H), 7.65 (broad s, 1H), 8.42 (d, 1H, J = 1 Hz). MS (CI): m/z 478 (MH^+, 75%), 480 ($MH^+ + 2$, 100%). HRFABMS calcd for $C_{22}H_{26}N_3O_2BrCl$, M_r 478.0897 (MH^+); found, 478.0885. Anal. ($C_{22}H_{25}N_3O_2BrCl\cdot0.5H_2O$) C, H, N.

(±)-4-(8-Chloro-6,11-dihydro-9-amino-10-iodo-5*H*-benzo-[5,6]cyclohepta[1,2-b]pyridin-11-yl)-1-piperidinecarboxylic Acid Ethyl Ester (6a). A mixture of iodine (26 g, 102.4 mmol), silver sulfate (32 g, 102.6 mmol), and 95% EtOH (1.8 L) was stirred at 25 °C for several minutes, and then, **5a** in 95% EtOH (1.8 L) was added to it and stirred at 25 °C for 3 days. The mixture was concentrated in vacuo, diluted with CH_2Cl_2, washed with 1 M NaOH(aq) and extracted with CH_2Cl_2. The combined CH_2Cl_2 layer was dried over anhydrous Na_2SO_4, filtered, and concentrated. Purification by chromatography on silica gel eluting with 40−70% EtOAc−Hexane afforded the product as a solid: 17.9 g, 35%. ^{1}H NMR (200 MHz, $CDCl_3$): δ 1.21 (t, 3H, J = 7 Hz), 1.30−1.65 (m, 4H), 2.30−2.80 (m, 4H), 2.87−3.09 (m, 1H), 3.22 (m, 1H), 3.60 (m, 1H), 3.95−4.23 (m, 2H), 4.10 (overlapping q, 2H, J = 7 Hz), 4.67 (s, 2H), 4.91 (d, 1H, J = 10 Hz), 7.08 (dd, 1H, J = 4 Hz, J = 8 Hz), 7.09 (overlapping s, 1H), 7.39 (d, 1H, J = 8 Hz), 8.40 (dd, 1H, J = 1 Hz, J = 4 Hz). MS (CI): m/z 526 (MH^+, 100%).

Compound **6a** was purified by HPLC using a Chiralpak AD column and 40% 2-propanol−60% hexane−0.2% diethylamine as eluent. The enatiomers **6a** were obtained as solids. (+)-**6a**: 7.0 g; 14% isolated yield; $[\alpha]_D^{23} = +78.2°$ (2.02 mg/2 mL, CH_2Cl_2). Anal. ($C_{22}H_{25}N_3O_2ClI\cdot0.9H_2O\cdot0.3C_6H_{14}$) C, H, N. HRFABMS calcd for $C_{22}H_{26}N_3O_2ClI$, M_r 526.0758 (MH^+); found, 526.0752. (−)-**6a**: 5.7 g; 11% isolated yield; $[\alpha]_D^{23} = -80.8°$ (4.58 mg/2 mL, CH_2Cl_2). HRFABMS calcd for $C_{22}H_{26}N_3O_2ClI$, M_r 526.0758 (MH^+); found, 526.0752.

(±)-4-(3-Bromo-8-chloro-6,11-dihydro-9-amino-10-iodo-5*H*-benzo[5,6]cyclohepta[1,2-b]pyridin-11-yl)-1-piperidinecarboxylic Acid Ethyl Ester (6b). Compound **6b** was prepared according to the procedure described for **6a**. Data for **6b**: solid, 10.7 g, 51%. ^{1}H NMR (200 MHz, $CDCl_3$): δ 1.20−1.75 (m, 4H), 1.29 (overlapping t, 3H, J = 7 Hz), 2.40 (m, 1H), 2.50−3.10 (m, 4H), 3.25 (m, 1H), 3.60 (m, 1H), 4.00−4.30 (m, 2H), 4.15 (overlapping q, 2H, J = 7 Hz), 4.69 (broad s, 2H), 4.91 (d, 1H, J = 10 Hz), 7.13 (s, 1H), 7.56 (d, 1H, J = 1 Hz), 8.48 (d, 1H, J = 1 Hz). MS (CI): m/z 604 (MH^+, 80%), 606 ($MH^+ + 2$, 100%). Anal. ($C_{22}H_{24}N_3O_2BrClI\cdot1.2H_2O\cdot0.3C_6H_{14}$) C, H, N.

(±)-4-(4-Chloro-3,6,7,12-tetrahydro-1-methyl-2-trimethylsilyl-pyrido[2′,3′:4,5]cyclohepta-[2,1-e]indol-12-yl)-1-piperidinecarboxylic Acid Ethyl Ester (7a). A mixture of **6a** (2 g, 3.8 mmol), $Pb(OAc)_2$ (256 mg, 1.14 mmol), Ph_3P (299 mg, 1.14 mmol), trimethylsilylpropyne (2.81 mL, 19 mmol), Na_2CO_3 (2.014 g, 19 mmol), ^{n}Bu_4NBr (1.225 g, 3.8 mmol), and dry DMF (70 mL) was stirred at 140 °C for 12 h under N_2. The mixture was cooled and concentrated in vacuo, diluted with CH_2Cl_2, washed with H_2O, dried over anhydrous $MgSO_4$, filtered, and concentrated. Purification by chromatography on silica gel eluting with 33% EtOAc−Hexane afforded the product as a solid: 1.5 g, 77%. ^{1}H NMR (200 MHz, $CDCl_3$): δ 0.45 (s, 9H), 1.00−1.78 (m, 5H), 1.24 (overlapping t, 3H, J = 7 Hz), 2.35−3.19 (m, 4H), 2.72 (overlapping s, 3H), 3.31 (m, 1H), 3.77 (m, 1H), 3.91−4.32 (m, 2H), 4.11 (overlapping q, 2H, J = 7 Hz), 5.18 (d, 1H, J = 10 Hz), 6.95−7.18 (m, 1H), 7.05 (overlapping s, 1H), 7.37 (d, 1H, J = 8 Hz), 7.91 (broad s, 1H), 8.38 (m, 1H). MS (CI): m/z 510 (MH^+, 100%). Anal. ($C_{28}H_{36}N_3O_2ClSi\cdot0.5H_2O$) C, H, N.

(±)-4-(4-Chloro-3,6,7,12-tetrahydro-1-propyl-2-trimethylsilyl-pyrido[2′,3′:4,5]cyclohepta-[2,1-e]indol-12-yl)-1-piperidinecarboxylic Acid Ethyl Ester (7b). Compound **7b** was prepared according to the procedure described for **7a**. Data for **7b**: solid, 382 mg, 74%. ^{1}H NMR (200 MHz, DMSO-d_6): δ 0.40 (s, 9H), 0.75−1.95 (m, 7H), 1.10 (overlapping t, 3H, J = 7 Hz), 1.20 (overlapping t, 3H, J = 7 Hz), 2.32−3.12 (m, 6H), 3.25 (m, 1H), 3.74 (m, 1H), 3.90−4.30 (m, 2H), 4.09 (overlapping q, 2H, J = 7 Hz), 4.91 (d, 1H, J = 10 Hz), 7.02 (s, 2H), 7.33 (d, 1H, J = 7.5 Hz), 7.90 (broad s, 1H), 8.33 (m, 1H). MS (CI): m/z 538 (MH^+, 100%). Anal. ($C_{30}H_{40}N_3O_2ClSi\cdot0.2C_6H_{14}$) C, H, N.

(±)-4-(4-Chloro-3,6,7,12-tetrahydro-1-butyl-2-trimethylsilyl-pyrido[2′,3′:4,5]cyclohepta-[2,1-e]indol-12-yl)-1-piperidinecarboxylic Acid Ethyl Ester (7c). Compound **7c** was prepared according to the procedure described for **7a**. Data for **7c**: solid, 380 mg, 73%. ^{1}H NMR (200 MHz, $CDCl_3$): δ 0.39 (s, 9H), 0.50−2.00 (m, 9H), 0.99 (overlapping t, 3H, J = 7 Hz), 1.24 (overlapping t, 3H, J = 7 Hz), 2.20−3.18 (m, 6H), 3.25 (m, 1H), 3.75 (m, 1H), 3.90−4.31 (m, 2H), 4.11 (overlapping q, 2H, J = 7 Hz), 4.93 (d, 1H, J = 10 Hz), 7.04 (m, 2H), 7.35 (d, 1H, J = 8 Hz), 7.93 (broad s, 1H), 8.35 (m, 1H). MS (CI): m/z 552 (MH^+, 100%). Anal. ($C_{31}H_{42}N_3O_2ClSi\cdot0.2C_6H_{14}$) C, H, N.

(±)-4-(9-Bromo-4-chloro-3,6,7,12-tetrahydro-1-methyl-2-trimethylsilyl-pyrido[2′,3′:4,5]cyclohepta-[2,1-e]indol-12-yl)-1-piperidinecarboxylic Acid Ethyl Ester (7d). Compound **7d** was prepared according to the procedure described for **7a**. Data for **7d**: solid, 2.15 g, 44%. ^{1}H NMR (200 MHz, DMSO-d_6): δ 0.40 (s, 9H), 1.02−1.73 (m, 5H), 1.28 (overlapping t, 3H, J = 7 Hz), 2.32−3.15 (m, 4H), 2.70 (overlapping s, 3H), 3.28 (m, 1H), 3.73 (m, 1H), 4.00−4.30 (m, 2H), 4.10 (overlapping q, 2H, J = 7 Hz), 5.15 (d, 1H, J = 10 Hz), 7.02 (s, 1H), 7.54 (d, 1H, J = 1 Hz), 7.94 (broad s, 1H), 8.41 (d, 1H, J = 1 Hz). MS (CI): m/z 588 (MH^+, 75%), 590 ($MH^+ + 2$, 100%). Anal. ($C_{28}H_{35}N_3O_2BrClSi\cdot0.2C_6H_{14}\cdot0.2H_2O$) C, H, N.

(+)-4-(4-Chloro-3,6,7,12-tetrahydro-1-hydroxymethyl-2-trimethylsilyl-pyrido[2′,3′:4,5]cyclohepta-[2,1-e]indol-12-yl)-1-piperidinecarboxylic Acid Ethyl Ester (+)-7e. Compound (+)-**7e** was prepared according to the procedure described for **7a**. Data for (+)-**7e**: solid, 2.05 g, 74%; mp =

123.7 °C. ^{1}H NMR (200 MHz, $CDCl_3$): δ 0.43 (broad s, 9H), 1.05−1.68 (m, 5H), 1.22 (overlapping t, 3H, J = 7 Hz), 2.68 (m, 2H), 2.80−3.11 (m, 2H), 3.30−3.51 (m, 1H), 3.68−3.92 (m, 1H), 4.00−4.30 (m, 2H), 4.12 (overlapping q, 2H, J = 7 Hz), 4.75 (d, 1H, J = 10 Hz), 4.65−5.12 (broad m, 1H), 4.88 (overlapping d, 1H, J = 13 Hz), 5.35 (d, 1H, J = 13 Hz), 7.00 (s, 1H), 7.04 (dd, 1H, J = 4 Hz, J = 8 Hz), 7.34 (d, 1H, J = 8 Hz), 8.04 (broad s, 1H), 8.21 (dd, 1H, J = 1 Hz, J = 4 Hz). MS (CI): m/z 526 (MH^+, 25%), 508 ($MH^+ - 18$, 100%); $[\alpha]_D^{25.0}$ = + 10.5° (3.62 mg/2 mL, CH_2Cl_2). Anal. ($C_{28}H_{36}N_3O_3ClSi \cdot 1.5CH_3OH$) C, H, N.

(−)-4-(4-Chloro-3,6,7,12-tetrahydro-1-hydroxymethyl-2-trimethylsilyl-pyrido[2′,3′:4,5]cyclohepta-[2,1-e]indol-12-yl)-1-piperidinecarboxylic Acid Ethyl Ester (−)-7e. Compound (−)-**7e** was prepared according to the procedure described for **7a**. Data for (−)-**7e**: solid, 3.5 g, 75%; mp = 118.6−143.7 °C. ^{1}H NMR (200 MHz, $CDCl_3$): δ 0.44 (s, 9H), 1.05−1.68 (m, 5H), 1.22 (overlapping t, 3H, J = 7 Hz), 2.56−3.11 (m, 4H), 3.30−3.50 (m, 1H), 3.66−3.90 (m, 1H), 3.98−4.28 (m, 2H), 4.10 (overlapping q, 2H, J = 7 Hz), 4.75 (d, 1H, J = 10 Hz), 4.88 (d, 1H, J = 13 Hz), 4.95 (m, 1H), 5.38 (d, 1H, J = 13 Hz), 7.00 (s, 1H), 7.04 (dd, 1H, J = 4 Hz, J = 8 Hz), 7.32 (d, 1H, J = 8 Hz), 8.09 (broad s, 1H), 8.21 (dd, 1H, J = 1 Hz, J = 4 Hz). MS (CI): m/z 526 (MH^+, 25%), 508 ($MH^+ - 18$, 100%); $[\alpha]_D^{21.5}$ = − 11.2° (4.30 mg/2 mL, CH_2Cl_2). Anal. ($C_{28}H_{36}N_3O_3ClSi \cdot 2.3H_2O$) C, H, N.

(±)-4-(4-Chloro-3,6,7,12-tetrahydro-1-methylpyrido[2′,3′:4,5]cyclohepta-[2,1-e]indol-12-yl)-1-piperidinecarboxylic Acid Ethyl Ester (8a). A mixture of **7a** (500 mg, 0.98 mmol), TBAF (1.0 M in THF, 2.94 mL, 2.94 mmol), and THF (5 mL) was stirred at 25 °C for 12 h. The mixture was concentrated in vacuo, diluted with CH_2Cl_2, washed with H_2O, dried over anhydrous $MgSO_4$, filtered, and concentrated to afford the product; 411 mg, 96%; mp = 186.7 °C. ^{1}H NMR (200 MHz, DMSO-d_6): δ 1.02−1.73 (m, 5H), 1.26 (overlapping t, 3H, J = 7 Hz), 2.32−3.50 (m, 5H), 2.65 (broad s, 3H), 3.78 (m, 1H), 3.92−4.33 (m, 2H), 4.10 (overlapping q, 2H, J = 7 Hz), 5.10 (m, 1H), 7.00 (broad s, 2H), 7.06 (s, 1H), 7.40 (m, 1H), 8.09 (m, 1H), 8.40 (m, 1H). MS (FAB): m/z 438 (MH^+, 100%). Anal. ($C_{25}H_{28}N_3O_2Cl \cdot CH_3OH \cdot 0.2C_6H_{14}$) C, H, N.

(±)-4-(4-Chloro-3,6,7,12-tetrahydro-1-propylpyrido[2′,3′:4,5]cyclohepta-[2,1-e]indol-12-yl)-1-piperidinecarboxylic Acid Ethyl Ester (8b). Compound **8b** was prepared according to the procedure described for **8a**. Data for **8b**: 333 mg, 100%; mp = 122.4 °C. ^{1}H NMR (200 MHz, $CDCl_3$): δ 0.75−2.05 (m, 7H), 1.10 (overlapping t, 3H, J = 7 Hz), 1.25 (overlapping t, 3H, J = 7 Hz), 2.30−3.20 (m, 6H), 3.33 (m, 1H), 3.76 (m, 1H), 3.90−4.33 (m, 2H), 4.11 (overlapping q, 2H, J = 7 Hz), 5.02 (d, 1H, J = 10 Hz), 7.00 (s, 1H), 7.06 (m, 2H), 7.40 (m, 1H), 8.10 (broad s, 1H), 8.39 (m, 1H). MS (FAB): m/z 466 (MH^+, 100%). Anal. ($C_{27}H_{32}N_3O_2Cl \cdot 1.3CH_3OH \cdot 0.5C_6H_{14}$) C, H, N.

(±)-4-(4-Chloro-3,6,7,12-tetrahydro-1-butylpyrido[2′,3′:4,5]cyclohepta-[2,1-e]indol-12-yl)-1-piperidinecarboxylic Acid Ethyl Ester (8c). Compound **8c** was prepared according to the procedure described for **8a**. Data for **8c**: 340 mg, 100%; mp = 111.8 °C. ^{1}H NMR (200 MHz, $CDCl_3$): δ 0.75−2.00 (m, 9H), 0.99 (overlapping t, 3H, J = 7 Hz), 1.27 (overlapping t, 3H, J = 7 Hz), 2.34−3.20 (m, 6H), 3.33 (m, 1H), 3.78 (m, 1H), 3.92−4.32 (m, 2H), 4.11 (overlapping q, 2H, J = 7 Hz), 5.01 (d, 1H, J = 10 Hz), 7.01 (s, 1H), 7.07 (m, 2H), 7.38 (d, 1H, J = 8 Hz), 8.10 (s, 1H), 8.37 (m, 1H). MS (FAB): m/z 480 (MH^+, 100%). Anal. ($C_{28}H_{34}N_3O_2Cl \cdot 0.6CH_3OH \cdot 0.4C_6H_{14}$) C, H, N.

(±)-4-(9-Bromo-4-chloro-3,6,7,12-tetrahydro-1-methylpyrido[2′,3′:4,5]cyclohepta -[2,1-e]indol-12-yl)-1-piperidinecarboxylic Acid Ethyl Ester (8d). Compound **8d** was prepared according to the procedure described for **8a**. Data for **8d**: 1.81 g, 96%. Compound **8d** was purified by HPLC using a Chiralpak AD column and 50% 2-propanol−50% hexane−0.2% diethylamine as eluent. The enatiomers **8d** were obtained as solids. (+)-**8d**: 884 mg; 47% isolated yield. ^{1}H NMR (200 MHz, $CDCl_3$): δ 0.80−1.80 (m, 5H), 1.24 (overlapping t, 3H, J = 7 Hz), 2.33−3.15 (m, 4H), 2.60 (overlapping s, 3H), 3.30 (m, 1H), 3.72 (m, 1H), 3.89−4.30 (m, 2H), 4.10 (overlapping q, 2H, J = 7 Hz), 5.05 (d, 1H, J = 10 Hz), 7.00 (s, 1H), 7.03 (s, 1H), 7.52 (d, 1H, J = 1 Hz), 8.09 (broad s, 1H), 8.41 (d, 1H, J = 1 Hz). MS (FAB): m/z 516 (MH^+, 80%), 518 (MH^++2, 100%); $[\alpha]_D^{24}$ = +37.9° (2.5 mg/2 mL, CH_3OH). Anal. ($C_{25}H_{27}N_3O_2BrCl \cdot 0.6C_6H_{14} \cdot 3H_2O$) C, H, N. (−)-**8d**: 725 mg; 38% isolated yield. ^{1}H NMR (200 MHz, $CDCl_3$): δ 1.00−1.72 (m, 5H), 1.24 (overlapping t, 3H, J = 7 Hz), 2.32−3.18 (m, 4H), 2.60 (overlapping s, 3H), 3.30 (m, 1H), 3.72 (m, 1H), 3.94−4.32 (m, 2H), 4.11 (overlapping q, 2H, J = 7 Hz), 5.05 (d, 1H, J = 10 Hz), 7.02 (s, 1H), 7.05 (s, 1H), 7.53 (s, 1H), 8.09 (broad s, 1H), 8.41 (s, 1H). MS (FAB): m/z 516 (MH^+, 80%), 518 ($MH^+ + 2$, 100%); $[\alpha]_D^{24}$ = − 33.78° (2.5 mg/2 mL, CH_3OH).

(±)-4-(4-Chloro-3,6,7,12-tetrahydro-1-methylpyrido[2′,3′:4,5]cyclohepta-[2,1-e]indol-12-yl)-1-piperidine (9a). Compound **8a** (498 mg, 0.98 mmol) was dissolved in EtOH (10 mL), KOH (3 M aqueous, 4.7 mL, 14.1 mmol) was added, and the reaction was brought up to reflux for 3 days. The mixture was cooled, concentrated in vacuo, diluted with CH_2Cl_2, washed with H_2O, dried over anhydrous $MgSO_4$, filtered, and concentrated. Purification by chromatography on silica gel eluting with 5% CH_3OH/95% CH_2Cl_2/0.1% NH_4OH afforded the product **9a** as a solid: 240 mg, 56%.

Compound **9a** was purified by HPLC using a Chiralpak AD column and 40% 2-propanol−60% hexane−0.2% diethylamine as eluent. The enatiomers **9a** were obtained as solids. (+)-**9a**: 110 mg; 26% isolated yield. ^{1}H NMR (200 MHz, $CDCl_3$): δ 1.05−2.20 (m, 6H), 2.30−3.45 (m, 7H), 2.65 (overlapping s, 3H), 3.65 (m, 1H), 5.14 (d, 1H, J = 10 Hz), 6.93−7.13 (m, 3H), 7.38 (d, 1H, J = 8 Hz), 8.04 (broad s, 1H), 8.35 (m, 1H). MS (CI): m/z 366 (MH^+, 100%), 368 ($MH^+ + 2$, 60%); $[\alpha]_D^{21.7}$ = + 66.0° (2.0 mg/2 mL, CH_3OH). Anal. ($C_{22}H_{24}N_3Cl \cdot 2H_2O$) C, H, N. (−)-**9a**: 92.8 mg; 22% isolated yield. ^{1}H NMR (200 MHz, $CDCl_3$): δ 1.10−2.20 (m, 6H), 2.30−3.50 (m, 7H), 2.67 (overlapping s, 3H), 3.66 (m, 1H), 5.16 (d, 1H, J = 10 Hz), 6.95−7.15 (m, 3H), 7.38 (d, 1H, J = 8 Hz), 8.05 (broad s, 1H), 8.36 (m, 1H). MS (CI): m/z 366 (MH^+, 100%), 368 ($MH^+ + 2$, 60%); $[\alpha]_D^{21.7}$ = − 82.4° (3.13 mg/2 mL, CH_3OH). Anal. ($C_{22}H_{24}N_3Cl \cdot 2H_2O$) C, H, N.

(±)-4-(4-Chloro-3,6,7,12-tetrahydro-1-propylpyrido[2′,3′:4,5]cyclohepta-[2,1-e]indol-12-yl)-1-piperidine (9b). Compound **8b** (275 mg, 0.6 mmol) was dissolved in EtOH (8 mL), concentrated HCl (15 mL) was added, and the reaction was refluxed for 12 h. The mixture was cooled, concentrated in vacuo, diluted with CH_2Cl_2, washed with H_2O, dried over anhydrous $MgSO_4$, filtered, and concentrated to afford the product **9b**; 147 mg, 63.4%. ^{1}H NMR (200 MHz, $CDCl_3$): 0.70−2.00 (m, 7H), 1.10 (overlapping t, 3H, J = 7 Hz), 2.05−3.45 (m, 10H), 3.71 (m, 1H), 5.05 (d, 1H, J = 10 Hz), 6.90−7.13 (m, 2H), 7.05 (overlapping s, 1H), 7.36 (d, 1H, J = 8 Hz), 8.09 (s, 1H), 8.37 (d, 1H, J = 1 Hz).

Compound **9b** was purified by HPLC using a Chiralpak AD column and 15% 2-propanol−85% hexane−0.2% diethylamine as eluent. The enatiomers **9b** were obtained as solids. (+)-**9b**: 44.8 mg; 19% isolated yield. ^{1}H NMR (200 MHz, $CDCl_3$): δ 0.84−2.30 (m, 7H), 1.10 (overlapping t, 3H, J = 7 Hz), 2.35−3.45 (m, 10H), 3.70 (m, 1H), 5.06 (d, 1H, J = 10 Hz), 6.92−7.15 (m, 2H), 7.02 (overlapping s, 1H), 7.36 (d, 1H, J = 8 Hz), 8.09 (m, 1H), 8.35 (m, 1H). MS (FAB): m/z 394 (MH^+, 100%); $[\alpha]_D^{23}$ = + 53.17° (2.5 mg/2 mL, CH_3OH). Anal. ($C_{24}H_{28}N_3Cl \cdot 0.4C_6H_{14} \cdot H_2O$) C, H, N. (−)-**9b**: 39.4 mg; 17% isolated yield. ^{1}H NMR (200 MHz, $CDCl_3$): δ 0.70−3.40 (m, 17H), 1.10 (overlapping t, 3H, J = 7 Hz), 3.71 (m, 1H), 5.07 (d, 1H, J = 10 Hz), 6.93−7.14 (m, 2H), 7.01 (overlapping s, 1H), 7.37 (d, 1H, J = 8 Hz), 8.10 (m, 1H), 8.35 (m, 1H). MS (FAB): m/z 394 (MH^+, 100%); $[\alpha]_D^{23}$ = − 67.79° (2.5 mg/2 mL, CH_3OH). Anal. ($C_{24}H_{28}N_3Cl \cdot CH_2Cl_2 \cdot 0.3C_6H_{14}$) C, H, N.

(±)-4-(4-Chloro-3,6,7,12-tetrahydro-1-butylpyrido[2′,3′:4,5]cyclohepta-[2,1-e]indol-12-yl)-1-piperidine (9c). Compound **9c** was prepared according to the procedure described for **9b**. Data for **9c**: 189.3 mg, 77.5%. ^{1}H NMR (200 MHz, $CDCl_3$): δ 0.99 (t, 3H, J = 7 Hz), 1.10−2.30 (m, 10H), 2.50 (m, 2H), 2.68−3.42 (m, 7H), 3.74 (m, 1H), 5.01 (d, 1H, J = 10 Hz), 6.92−7.14 (m, 2H), 7.03 (overlapping s, 1H), 7.35 (d, 1H,

J = 8 Hz), 8.09 (s, 1H), 8.35 (m, 1H). Compound **9c** was purified by HPLC using a Chiralpak AD column and 10% 2-propanol−90% hexane−0.2% diethylamine as eluent. The enatiomers **9c** were obtained as solids. (+)-**9c**: 70 mg; 29% isolated yield. ^{1}H NMR (200 MHz, $CDCl_3$): δ 1.10−2.20 (m, 10H), 1.00 (overlapping t, 3H, J = 7 Hz), 2.52 (m, 2H), 2.75−3.43 (m, 7H), 3.79 (m, 1H), 5.05 (d, 1H, J = 10 Hz), 6.99−7.18 (m, 2H), 7.04 (overlapping s, 1H), 7.39 (d, 1H, J = 8 Hz), 8.11 (s, 1H), 8.39 (d, 1H, J = 1 Hz). MS (FAB): m/z 408 (MH^+, 100%); $[\alpha]_D^{23}$ = + 88.78° (2.5 mg/2 mL, CH_3OH). Anal. ($C_{25}H_{30}N_3Cl\cdot0.2C_6H_{14}\cdot2.2H_2O$) C, H, N. (−)-**9c**: 62 mg; 25% isolated yield. ^{1}H NMR (200 MHz, $CDCl_3$): δ 1.10−2.15 (m, 10H), 0.99 (overlapping t, 3H, J = 7 Hz), 2.49 (m, 2H), 2.70−3.40 (m, 7H), 3.75 (m, 1H), 5.03 (d, 1H, J = 10 Hz), 6.95−7.15 (m, 2H), 7.03 (overlapping s, 1H), 7.36 (d, 1H, J = 8 Hz), 8.10 (broad s, 1H), 8.36 (d, 1H, J = 1 Hz). MS (FAB): m/z 408 (MH^+, 100%); $[\alpha]_D^{23}$ = − 81.50° (2.5 mg/2 mL, CH_3OH). Anal. ($C_{25}H_{30}N_3Cl\cdot0.4C_6H_{14}\cdot2.2H_2O$) C, H, N.

(+)-4-(9-Bromo-4-chloro-3,6,7,12-tetrahydro-1-methylpyrido[2′,3′:4,5]cyclohepta-[2,1-e]indol-12-yl)-1-piperidine [(+)-9d]. Compound (+)-**9d** was prepared according to the procedure described for **9b**. Data for (+)-**9d**: 180 mg, 23%. ^{1}H NMR (200 MHz, $CDCl_3$): δ 1.10−2.25 (m, 6H), 2.35−3.45 (m, 7H), 2.67 (overlapping s, 3H), 3.74 (m, 1H), 5.09 (d, 1H, J = 10 Hz), 7.03 (s, 1H), 7.06 (s, 1H), 7.56 (m, 1H), 8.11 (broad s, 1H), 8.42 (m, 1H). MS (FAB): m/z 444 (MH^+, 75%), 446 (MH^+ + 2, 100%).

(+)-4-(4-Chloro-3,6,7,12-tetrahydro-1-methylpyrido[2′,3′:4,5]cyclohepta-[2,1-e]indol-12-yl)-1-(4-pyridinylacetyl)piperidine N1-Oxide [(+)-10a]. A mixture of (+)-**9a** (75 mg, 0.2 mmol), pyridyl acetic acid N-oxide (31 mg, 0.2 mmol), HOBt (27 mg, 0.2 mmol), DEC (38.3 mg, 0.2 mmol), and dry DMF (5 mL) was stirred at 25 °C for 12 h. The mixture was concentrated in vacuo, diluted with CH_2Cl_2, washed with 1 M NaOH(aq), and dried over anhydrous $MgSO_4$ to afford the product after preparative plate chromatography (silica gel, 5% MeOH/CH_2Cl_2 saturated with NH_4OH): off-white solid, 60 mg, 60%; mp = 183.6 °C. ^{1}H NMR (200 MHz, $CDCl_3$): δ 0.70−2.30 (m, 5H), 2.32−4.05 (m, 9H), 2.75 (overlapping s, 3H), 4.64 (m, 1H), 5.33 (m, 1H), 7.09 (s, 2H), 7.20 (m, 3H), 7.49 (m, 1H), 8.20 (m, 3H), 8.60 (m, 1H); $[\alpha]_D^{21.7}$ = + 55.8° (2.40 mg/2 mL, MeOH). MS (FAB): m/z 501 (MH^+, 100%). Anal. ($C_{29}H_{29}N_4O_2Cl\cdot0.4C_6H_{14}\cdot3H_2O$) C, H, N.

(−)-4-(4-Chloro-3,6,7,12-tetrahydro-1-methylpyrido[2′,3′:4,5]cyclohepta-[2,1-e]indol-12-yl)-1-(4-pyridinylacetyl)piperidine N1-Oxide [(−)-10a]. Compound (−)-**10a** was prepared according to the procedure described for (+)-**10a**. Data for (−)-**10a**: white solid, 33 mg, 41%; mp = 187.3 °C. ^{1}H NMR (200 MHz, $CDCl_3$): δ 0.70−2.26 (m, 5H), 2.32−4.02 (m, 9H), 2.72 (overlapping s, 3H), 4.63 (m, 1H), 5.30 (m, 1H), 7.08 (s, 2H), 7.20 (m, 3H), 7.47 (m, 1H), 8.18 (m, 3H), 8.59 (m, 1H); $[\alpha]_D^{21.7}$ = −52.2° (1.84 mg/2 mL, MeOH). MS (FAB): m/z 501 (MH^+, 100%). Anal. ($C_{29}H_{29}N_4O_2Cl\cdot0.4C_6H_{14}\cdot3H_2O$) C, H, N.

(+)-4-(4-Chloro-3,6,7,12-tetrahydro-1-propylpyrido[2′,3′:4,5]cyclohepta-[2,1-e]indol-12-yl)-1-(4-pyridinylacetyl)piperidine N1-Oxide [(+)-10b]. Compound (+)-**10b** was prepared according to the procedure described for (+)-**10a**. Data for (+)-**10b**: light brown foam; 31 mg, 60%; mp = 146.8 °C. ^{1}H NMR (200 MHz, $CDCl_3$): δ 0.74−2.25 (m, 7H), 1.08 (overlapping t, 3H, J = 7 Hz), 2.50 (m, 2H), 2.70−3.41 (m, 5H), 3.48−4.00 (m, 2H), 3.62, 3.69 (two overlapping s, acetyl CH_2, 2H), 4.59 (m, 1H), 5.02 (d, 1H, J = 10 Hz), 6.92−7.36 (m, 5H), 7.42 (m, 1H), 8.17 (m, 2H), 8.27 (s, 1H), 8.41 (broad s, 1H). $[\alpha]_D^{23}$ = + 45.04° (10 mg/2 mL, MeOH). MS (FAB): m/z 529 (MH^+, 100%). Anal. ($C_{31}H_{33}N_4O_2Cl\cdot3H_2O$) C, H, N.

(−)-4-(4-Chloro-3,6,7,12-tetrahydro-1-propylpyrido[2′,3′:4,5]cyclohepta-[2,1-e]indol-12-yl)-1-(4-pyridinylacetyl)piperidine N1-Oxide [(−)-10b]. Compound (−)-**10b** was prepared according to the procedure described for (+)-**10a**. Data for (−)-**10b**: light brown foam, 7 mg, 56%; mp = 143.8 °C. ^{1}H NMR (200 MHz, $CDCl_3$): δ 0.70−2.70 (m, 9H), 1.08 (overlapping t, 3H, J = 7 Hz), 2.73−3.42 (m, 5H), 3.48−3.95 (m, 2H), 3.65, 3.69 (two overlapping s, acetyl CH_2, 2H), 4.60 (m, 1H), 5.03 (d, 1H, J = 10 Hz), 7.00−7.26 (m, 5H), 7.43 (m, 1H), 8.18 (t, 2H, J = 8 Hz), 8.34 (m, 1H), 8.40 (m, 1H); $[\alpha]_D^{23}$ = − 60.42° (7.5 mg/2 mL, MeOH). MS (FAB): m/z 529 (MH^+, 100%). Anal. ($C_{31}H_{33}N_4O_2Cl\cdot0.1C_6H_{14}\cdot3.5H_2O$) C, H, N.

(+)-4-(4-Chloro-3,6,7,12-tetrahydro-1-butylpyrido[2′,3′:4,5]cyclohepta-[2,1-e]indol-12-yl)-1-(4-pyridinylacetyl)piperidine N1-Oxide [(+)-10c]. Compound (+)-**10c** was prepared according to the procedure described for (+)-**10a**. Data for (+)-**10c**: off-white solid, 43 mg, 40%; mp = 146.1 °C. ^{1}H NMR (200 MHz, $CDCl_3$): δ 0.70−2.24 (m, 9H), 0.98 (overlapping t, 3H, J = 7 Hz), 2.31−3.45 (m, 7H), 3.50−3.96 (m, 2H), 3.62, 3.69 (two overlapping s, acetyl CH_2, 2H), 4.60 (m, 1H), 5.02 (d, 1H, J = 10 Hz), 6.96−7.25 (m, 5H), 7.41 (m, 1H), 8.18 (m, 2H), 8.28 (m, 1H), 8.40 (m, 1H); $[\alpha]^{23}_D$ = + 50.23° (2.5 mg/2 mL, MeOH). MS (FAB): m/z 543 (MH^+, 100%). Anal. ($C_{32}H_{35}N_4O_2Cl\cdot2H_2O$) C, H, N.

(−)-4-(4-Chloro-3,6,7,12-tetrahydro-1-butylpyrido[2′,3′:4,5]cyclohepta-[2,1-e]indol-12-yl)-1-(4-pyridinylacetyl)piperidine N1-Oxide [(−)-10c]. Compound (−)-**10c** was prepared according to the procedure described for (+)-**10a**. Data for (−)-**10c**: yellow foam, 48 mg, 69%; mp = 149.3 °C. ^{1}H NMR (200 MHz, $CDCl_3$): δ 0.60−2.10 (m, 9H), 0.97 (overlapping t, 3H, J = 7 Hz), 2.30−3.45 (m, 7H), 3.50−3.96 (m, 2H), 3.61, 3.66 (two overlapping s, acetyl CH_2, 2H), 4.60 (m, 1H), 5.00 (d, 1H, J = 10 Hz), 6.92−7.25 (m, 5H), 7.40 (m, 1H), 8.18 (m, 2H), 8.24 (m, 1H), 8.39 (m, 1H); $[\alpha]_D^{23}$ = − 87.74° (2.5 mg/2 mL, MeOH). MS (FAB): m/z 543 (MH^+, 100%). Anal. ($C_{32}H_{35}N_4O_2Cl\cdot0.4CH_2Cl_2\cdot3H_2O$) C, H, N.

(+)-4-(9-Bromo-4-chloro-3,6,7,12-tetrahydro-1-methylpyrido[2′,3′:4,5]-cyclohepta[2,1-e]indol-12-yl)-1-(4-pyridinylacetyl)piperidine N1-Oxide [(+)-10d]. Compound (+)-**10d** was prepared according to the procedure described for (+)-**10a**. Data for **(+) 10d**: yellow solid; 66 mg, 55%; mp = 188.6−196.5 °C (dec). ^{1}H NMR (200 MHz, $CDCl_3$): δ 0.74−1.88 (m, 5H), 2.31−2.72 (m, 2H), 2.58 (overlapping s, 3H), 2.75−3.19 (m, 3H), 3.30 (m, 1H), 3.50−3.95 (m, 1H), 3.63, 3.68 (two overlapping s, acetyl CH_2, 2H), 4.60 (m, 1H), 5.03 (d, 1H, J = 10 Hz), 7.05 (m, 2H), 7.15 (t, 2H, J = 7 Hz), 7.55 (s, 1H), 8.16 (m, 3H), 8.42 (m, 1H); $[\alpha]_D^{24}$ = + 41.37° (2.5 mg/2 mL, MeOH). MS (FAB): m/z 579 (MH^+, 65%), 581 (MH^+ + 2, 88%), 583 (MH^+ + 4, 32%), 361 (100%). Anal. ($C_{29}H_{28}N_4O_2BrCl\cdot0.5C_6H_{14}\cdot4.5H_2O$) C, H, N.

(+)-4-(4-Chloro-3,6,7,12-tetrahydro-pyrido[2′,3′:4,5]cyclohepta-[2,1-e]indol-12-yl)-1-piperidine ((+)-11). Compound (+)-**11** was prepared according to the procedure described for **9a**. Data for (+)-**11**: 330 mg, 29%. ^{1}H NMR (200 MHz, $CDCl_3$): δ 1.02−1.58 (m, 5H), 1.95 (m, 1H), 2.21−2.60 (m, 2H), 2.80−3.10 (m, 4H), 3.31−3.71 (m, 2H), 4.49 (d, 1H, J = 10 Hz), 6.77 (d, 1H, J = 4 Hz), 6.97 (s, 1H), 7.08 (dd, 1H, J = 4 Hz, J = 8 Hz), 7.19 (d, 1H, J = 4 Hz), 7.37 (m, 1H), 8.31 (dd, 1H, J = 1 Hz, J = 4 Hz), 8.47 (m, 1H); $[\alpha]_D^{24}$ = − 13.2° (4.63 mg/2 mL, CH_2Cl_2). MS (CI): m/z 352 (MH^+, 100%). Anal. ($C_{21}H_{22}N_3Cl\cdot0.2C_6H_{14}\cdot1.4H_2O$) C, H, N.

(+)-4-(4-Chloro-3,6,7,12-tetrahydropyrido[2′,3′:4,5]cyclohepta-[2,1-e]indol-12-yl)-1-(4-pyridinylacetyl)piperidine N1-Oxide [(+)-12]. Compound (+)-**12** was prepared according to the procedure described for (+)-**10a**. Data for (+)-**12**: solid, 345 mg, 90%; mp = 179.3 °C. ^{1}H NMR (200 MHz, $CDCl_3$): δ 1.00−1.70 (m, 4H), 2.10 (m, 1H), 2.32−2.68 (m, 2H), 2.78−3.12 (m, 3H), 3.30−3.90 (m, 2H), 3.65 (overlapping s, 2H), 4.52 (m, 2H), 6.72 (m, 1H), 6.96−7.31(m, 4H), 7.02 (overlapping s, 1H), 7.42 (d, 1H, J = 8 Hz), 8.15 (m, 2H), 8.34 (m, 1H), 8.82 (d, 1H, J = 10 Hz). MS (FAB): m/z 487 (MH^+, 16%), 471 (MH^+ − 16, 100%). Anal. ($C_{28}H_{27}N_4O_2Cl\cdot1.6CH_2Cl_2\cdot1.5H_2O$) C, H, N.

(±)-4-(4-Chloro-3,6,7,12-tetrahydro-1,3-dimethyl-2-trimethylsilyl-pyrido[2′,3′:4,5]cyclohepta-[2,1-e]indol-12-yl)-1-piperidinecarboxylic Acid Ethyl Ester (13). To a solution of **7a** (203 mg, 0.46 mmol) in anhydrous THF (10 mL) was added NaH (200 mg, 60% in mineral oil, 5 mmol). After gas evolution ceased, MeI (0.035 mL, 0.56 mmol) was added and the mixture was stirred at room temperature for 4 days. The mixture was quenched with H_2O, concentrated in vacuo, diluted with CH_2Cl_2, washed with brine, dried over anhydrous $MgSO_4$, filtered, and concentrated. Purification by preparative TLC eluting with 25% EtOAc−Hexane afforded the product

as a white solid; 47.8 mg, 20%. ^{1}H NMR (200 MHz, DMSO-d_6): δ 0.48 (s, 9H), 0.81−1.7 (m, 5H), 1.15 (overlapping t, 3H, J = 7 Hz), 2.25−3.05 (m, 4H), 2.63 (overlapping s, 3H), 3.15−4.13 (m, 6H), 4.05 (overlapping s, 3H), 5.13 (d, 1H, J = 10 Hz), 7.10 (s, 1H), 7.20 (dd, 1H, J = 4 Hz, J = 8 Hz), 7.50 (d, 1H, J = 8 Hz), 8.33 (m, 1H). MS (FAB): m/z 524 (MH^+, 100%), 526 ($MH^+ + 2$, 43%). Anal. ($C_{29}H_{38}N_3O_2ClSi \cdot 0.5C_6H_{14}$) C, H.

(±)-4-(4-Chloro-3,6,7,12-tetrahydro-1,3-dimethyl-pyrido-[2′,3′:4,5]cyclohepta-[2,1-e]indol-12-yl)-1-piperidinecarboxylic Acid Ethyl Ester. This compound was also produced; 69.5 mg, 33%.

Desilylation of 13. (±)-4-(4-Chloro-3,6,7,12-tetrahydro-1,3-dimethyl- pyrido[2′,3′:4,5]cyclohepta-[2,1-e]indol-12-yl)-1-piperidinecarboxylic Acid Ethyl Ester. This compound was prepared according to the procedure described for **8a**. Data: tan solid, 42.7 mg, 100%. ^{1}H NMR (200 MHz, DMSO-d_6): δ 0.81−1.68 (m, 5H), 1.18 (overlapping t, 3H, J = 7 Hz), 2.4−3.05 (m, 4H), 2.49 (overlapping s, 3H), 3.15−4.13 (m, 6H), 3.99 (overlapping s, 3H), 4.96 (d, 1H, J = 10 Hz), 7.06 (s, 1H), 7.10 (s, 1H), 7.20 (dd, 1H, J = 4 Hz, J = 8 Hz), 7.50 (d, 1H, J = 8 Hz), 8.33 (m, 1H).

Hydrolysis of Desilylated 13. (±)-4-(4-Chloro-3,6,7,12-tetrahydro-1,3-dimethyl-pyrido[2′,3′:4,5]cyclohepta-[2,1-e]indol-12-yl)-1-piperidine. This compound was prepared according to the procedure described for **9a**. Data: tan solid; 68 mg, 78%. ^{1}H NMR (200 MHz, $CDCl_3$): δ 0.6−2.0 (m, 5H), 2.20−3.74 (m, 9H), 2.55 (overlapping s, 3H), 3.96 (s, 3H), 5.07 (d, 1H, J = 10 Hz), 6.66 (s, 1H), 6.92 (s, 1H), 6.98 (dd, 1H, J = 4 Hz, J = 8 Hz), 7.30 (d, 1H, J = 8 Hz), 8.29 (m, 1H). MS (FAB): m/z 380 (MH^+, 100%), 382 ($MH^+ + 2$, 34%). HRFABMS calcd for $C_{23}H_{27}N_3Cl$, M_r 380.1894 (MH^+); found, 380.1895.

(±)-4-(4-Chloro-3,6,7,12-tetrahydro-1,3-dimethylpyrido-[2′,3′:4,5]cyclo-hepta[2,1-e]indol-12-yl)-1-(4-pyridinylacetyl)piperidine N1-Oxide (14). Compound **14** was prepared according to the procedure described for **10a**. Data for **14**: 5.3 mg, 7%. ^{1}H NMR (200 MHz, $CDCl_3$): δ 0.5−2.6 (m, 7H), 2.69 (s, 3H), 2.75−4.10 (m, 7H), 4.00 (overlapping s, 3H), 4.55 (m, 1H), 5.32 (m, 1H), 6.78 (s, 1H), 7.0 (s, 1H), 7.3 (m, 2H), 7.64 (m, 1H), 8.02 (d, 1H, J = 8 Hz), 8.19 (m, 2H), 8.70 (m, 1H). MS (FAB): m/z 515 (MH^+, 100%), 517 ($MH^+ + 2$, 40%). HRFABMS calcd for $C_{30}H_{32}N_4O_2Cl$, M_r 515.2214 (MH^+); found, 515.2226.

4-(3-Bromo-8-chloro-5,6-dihydro-9-amino-10-iodo-11H-benzo[5,6]cyclohepta[1,2-b]pyridin-11-ylidene)-1-piperidinecarboxylic Acid Ethyl Ester (17). Compound **17** was prepared according to the procedure described for **6a**. Data for **17**: 3.48 g, 94%. ^{1}H NMR (200 MHz, $CDCl_3$): δ 1.21 (t, 3H, J = 7 Hz), 1.85−2.49 (m, 4H), 2.79 (m, 2H), 2.96−3.49 (m, 4H), 3.55−3.90 (m, 2H), 4.08 (q, 2H, J = 7 Hz), 5.18 (broad s, 2H), 7.31 (s, 1H), 7.78 (m, 1H), 8.55 (s, 1H). MS (FAB): m/z 602 (MH^+, 75%), 604 ($MH^+ + 2$, 100%).

4-(9-Bromo-4-Chloro-3,6,7,12-tetrahydro-1-methyl-2-trimethylsilyl-pyrido[2′,3′:4,5]cyclohepta-[2,1-e]indol-12-ylidene)-1-piperidinecarboxylic Acid Ethyl Ester (18). Compound **18** was prepared according to the procedure described for **7a**. Data for **18**: 717 mg, 34%. ^{1}H NMR (200 MHz, $CDCl_3$): 0.40 (s, 9H), 1.29 (m, 3H), 2.10 (m, 2H), 2.35−3.18 (m, 6H), 2.49 (overlapping s, 3H), 3.18−3.42 (m, 1H), 3.42−3.72 (m, 1H), 3.72−4.30 (m, 2H), 4.18 (overlapping q, 2H, J = 7 Hz), 7.09 (s, 1H), 7.51 (s, 1H), 7.94 (s, 1H), 8.49 (s, 1H). MS (FAB): m/z 585 (MH^+, 85%), 587 ($MH^+ + 2$, 100%).

(±)-4-(9-Bromo-4-Chloro-3,6,7,12-tetrahydro-1-methyl-pyrido[2′,3′:4,5]cyclohepta-[2,1-e]indol-12-ylidene)-1-piperidinecarboxylic Acid Ethyl Ester (19). Compound **19** was prepared according to the procedure described for **8a**. Data for **19**: 618 mg, 63%. ^{1}H NMR (200 MHz, $CDCl_3$): δ 1.29 (m, 3H), 2.10 (m, 2H), 2.39 (s, 3H), 3.59 (m, 2H), 2.68−3.13 (m, 4H), 3.20−4.20 (m, 4H), 4.15 (overlapping q, 2H, J = 7 Hz), 6.99 (s, 1H), 7.10 (s, 1H), 7.50 (s, 1H), 8.07 (s, 1H), 8.48 (m, 1H). MS (FAB): m/z 514 (MH^+, 90%), 516 ($MH^+ + 2$, 100%). Anal. ($C_{25}H_{25}N_3O_2BrCl \cdot 1.2CH_2Cl_2 \cdot 0.3C_6H_{14}$) C, H, N.

(±)-4-(9-Bromo-4-Chloro-3,6,7,12-tetrahydro-1-propyl-pyrido[2′,3′:4,5]cyclohepta-[2,1-e]indol-12-ylidene)-1-piperidine (20). Compound **20** was prepared according to the procedure described for **9a**. Data for **20**: 353 mg, 72%. ^{1}H NMR (200 MHz, $CDCl_3$): δ 1.8−3.80 (m, 13H), 2.40 (overlapping s, 3H), 6.99 (s, 1H), 7.10 (s, 1H), 7.50 (s, 1H), 8.09 (broad s, 1H), 8.49 (s, 1H). MS (FAB): m/z 442 (MH^+, 90%), 444 ($MH^+ + 2$, 100%). HRFABMS calcd for $C_{22}H_{22}N_3BrCl$, M_r 442.0686 (MH^+); found, 442.0694.

4-(9-Bromo-4-chloro-3,6,7,12-tetrahydro-1-methylpyrido-[2′,3′:4,5]cyclo-hepta[2,1-e]indol-12-ylidine)-1-(4-pyridinylacetyl)piperidine N1-Oxide (21). Compound **21** was prepared according to the procedure described for **10a**. Data for **21**: tan solid, 264 mg, 60%; mp = 202.7 °C (dec). ^{1}H NMR (200 MHz, $CDCl_3$): δ 2.08 (m, 2H), 2.30 (s, 3H), 2.37−4.50 (m, 10H), 3.65, 3.71 (two overlapping s, acetyl CH_2, 2H), 6.94 (s, 1H), 7.03 (s, 1H), 7.24 (m, 2H), 7.52 (d, 1H, J = 10 Hz), 8.12 (s, 1H), 8.23 (m, 2H), 8.45 (m, 1H). MS (FAB): m/z 577 (MH^+, 90%), 579 ($MH^+ + 2$, 100%). Anal. ($C_{29}H_{26}N_4O_2BrCl \cdot 1.6H_2O$) C, H, N.

(+)-4-(10-Bromo-8-chloro-6,11-dihydro-5H-benzo[5,6]-cyclohepta[1,2-b]pyridin-11(R)-yl)-1-(4-piperidinylacetyl)-piperidine N1-Oxide (22b). Compound **22b** was prepared from (+)-**5b** according to the procedures described in ref 8a. Data for **22b**: off-white solid; 270 mg, 50%; mp = 139−149 °C. ^{1}H NMR (300 MHz, $CDCl_3$): δ 1.20−1.67 (m, 5H), 2.45 (m, 2H), 2.75−3.10 (m, 3H), 3.30 (m, 1H), 3.80 (m, 1H), 3.68 (s, 2H), 4.58 (m, 1H), 4.98 (d, 1H, J = 10 Hz), 7.15 (m, 4H), 7.43 (m, 1H), 7.48 (broad s, 1H), 8.18 (d, 2H, J = 7 Hz), 8.41 (m, 1H). MS (FAB): m/z 526 (MH^+, 68%), 528 ($MH^+ + 2$, 92%), 393 (100%). Anal. ($C_{26}H_{25}N_3O_2Br \cdot 3.2H_2O$) C, H, N.

References

(1) (a) Barbacid, M. ras Genes. *Annu. Rev. Biochem.* **1987**, *56*, 779−827. (b) Der, C.; Cox, A. D. Isoprenoid Modification and Plasma Membrane Association: Critical Factors for Ras Oncogenicity. *Cancer Cells* **1991**, *3*, 331−340. (c) Willumsen, B. M.; Norris, K.; Papageorge, A. G.; Hubbert, N. L.; Lowry, D. R. Harvey Murine Sarcoma Virus p21 Ras Protein: Biological and Biochemical Significance of the Cysteine Nearest the Carboxyl Terminus. *EMBO J.* **1984**, *3*, 2581−2585. (d) Lowry, D. R.; Willumsen, B. M. New Clue to the Ras Lipid Glue. *Nature* (*London*) **1989**, *341*, 384−385. (e) Gibbs, J. B. Ras C-Terminal Processing Enzyme- New Drug Targets. *Cell* **1991**, *65*, 1−4. (f) Khosravi-Far, R.; Cox, A. D.; Kato, K.; Der, C. J. Protein Prenylation: Key to Ras Function and Cancer Intervention? *Cell Growth Differ.* **1992**, *3*, 461−469.

(2) (a) Barbacid, M. ras Oncogenes: their role in neoplasia. *Eur. J. Clin. Invest.* **1990**, *20*, 225−235. (b) Cox, A. D.; Der, C. J. Farnesyl transferase inhibitors and cancer treatment: targeting simply Ras? *Biochim. Biophys. Acta* **1997**, *1333*, F51−F71. (c) Prendergast, G. C.; Rane, N. Farnesyltransferase inhibitors: mechanism and applications. *Curr. Opin. Cell Biol.* **2000**, *12*, 166−173. (d) Ashar, H. R.; James, L.; Gray, K.; Carr, D.; Black, S.; Armstrong, L.; Bishop, W. R.; Kirschmeier, P. Farnesyl transferase inhibitors block the farnesylation of CENP-E and CENP-F and alter the association of CENP-E with the microtubules. *J. Biol. Chem.* **2000**, *275*, 30451−30457. (e) Ashar, H. R.; James, L. J.; Gray, K.; Carr, D. M.; McGuirk, M.; Maxwell, E.; Black, S.; Armstrong, L.; Doll, R. J.; Taveras, A. G.; Bishop, W. R.; Kirschmeier, P. T. The farnesyl transferase inhibitor SCH 66336 induces a G(2) → M or G(1) pause in sensitive human tumor cell lines. *Exp. Cell Res.* **2001**, *262* (1), 17−27. (f) Tamanoi, F.; Kato-Stankiewicz, J.; Jiang, C.; Machado, I.; Thapar, N. Farnesylated proteins and cell cycle progression. *J. Cell. Biochem.* **2001**, *Suppl. 37*, 64−70.

(3) (a) James, G. L.; Goldstein, J. L.; Brown, M. S.; Rawson, T. E.; Somers, T. C.; McDowell, R. S.; Crowley, C.; Lucas, B.; Levinson, A.; Masters, J. C. Benzodiazepine Peptidomimetics: Potent Inhibitors of Ras Farnesylation in Animal Cells. *Science* **1993**, *260*, 1937−1942. (b) Kohl, N. E.; Mosser, S. D.; DeSolms, J.; Giuliani, E. A.; Pompliano, D. L.; Graham, S. L.; Smith, R. L.; Scolnick, E. M.; Oliff, A.; Gibbs, J. B. Selective Inhibition of ras-Dependent Transformation by a Farnesyltransferase Inhibitor. *Science* **1993**, *260*, 1934−1937. (c) Garcia, A. M.; Rowell, C.; Ackermann, K.; Kowalczyk, J. J.; Lewis, M. D. Peptidomimetic Inhibitors of Ras Farnesylation and Function in Whole Cells. *J. Biol. Chem.* **1993**, *268*, 18415−18418. (d) Vogt, A.; Qian, Y.; Blaskovich, M. A.; Fossum, R. D.; Hamilton, A. D.; Sebti, S. M. A Non-Peptidic Mimetic of Ras-CAAX: Selective Inhibition of Farnesyltransferase and Ras Processing. *J. Biol. Chem.* **1995**, *270*, 660−664. (e) Kohl, N. E.; Wilson, F. R.; Mosser, S. D.; Giuliani, E.; DeSolms, S. J.; Conner, M. W.; Anthony, N. J.; Holtz, W. J.; Gomez, R. P.; Lee, T.-J.; Smith, R. L.; Graham, S. L.; Hartman, G. D.; Gibbs, J. B.; Oliff, A. Protein Farnesyltrans-

ferase Inhibitors Block the Growth of ras-Dependent Tumors in Nude Mice. *Proc. Natl. Acad. Sci. U.S.A.* **1994**, *91*, 9141−9145. (f) Casey, P. J.; Solski, P. A.; Der, C. I.; Buss, J. E. p21 Ras is Modified by a Farnesyl Isoprenoid. *Proc. Natl. Acad. Sci. U.S.A.* **1989**, *86*, 8323−8327.

(4) (a) Park, H. W.; Boduluri, S. R.; Moomaw, J. F.; Casey, P. J.; Beese, L. S. Crystal Structure of Protein Farnesyltransferase at 2.25 Angstrom Resolution. *Science* **1997**, *275*, 1800−1804. (b) Long, S. B.; Casey, P. J.; Beese, L. S. Co-Crystal Structure of Protein Farnesyltransferase Complexed with a Farnesyl Diphosphate Substrate. *Biochemistry* **1998**, *37*, 9612−9618. (c) Strickland, C. L.; Windsor, W. T.; Syto, R.; Wang, L.; Bond, R.; Wu, Z.; Schwartz, J.; Le, H. V.; Beese, L. S.; Weber, P. C. Crystal Structure of Farnesyl Protein Transferase Complexed with a CaaX Peptide and Farnesyl Diphosphate Analogue. *Biochemistry* **1998**, *37*, 16601−16611.

(5) (a) Reiss, Y.; Goldstein, J. L.; Seabra, M. C.; Casey, P. J.; Brown, M. S. Inhibition of Purified p21 Ras Farnesyl Protein Transferase by Cys-AAX Tetrapeptides. *Cell* **1990**, *62*, 81−88. (b) Hancock, J. F.; Magee, A. I.; Childs, J. E.; Marshall, C. J. All Ras Proteins are Polyisoprenylated but Only Some are Palmitoylated. *Cell* **1989**, *57*, 1176−1177.

(6) Rotella, D. P. An Update on Cox-2 and Farnesyltransferase Inhibitor Development. *Curr. Opin. Drug Discovery Dev.* **1998**, *1*, 165−174.

(7) (a) Bishop, W. R.; Bond, R.; Petrin, J.; Wang, L.; Patton, R.; Doll, R.; Njoroge, N.; Windsor, W.; Syto, R.; Schwartz, J.; Carr, D.; James, L.; Kirschmeier, P. Novel Tricyclic Inhibitors of Farnesyl Protein Transferase. *J. Biol. Chem.* **1995**, *270*, 30611−30618. (b) Mallams, A. K.; Njoroge, F. G.; Doll, R. J.; Snow, M. E.; Kaminski, J. J.; Rossman, R.; Vibulbhan, B.; Bishop, W. R.; Kirschmeier, P.; Liu, M.; Bryant, M. S.; Alvarez, C.; Carr, D.; James, L.; King, I.; Li, Z.; Lin, C.-C.; Nardo, C.; Petrin, J.; Remiszewski, S.; Taveras, A.; Wang, S.; Wong, J.; Catino, J.; Girijavallabhan, V.; Ganguly, A. K. Antitumor 8-Chlorobenzocycloheptapyridines: a New Class of Selective, Nonpeptidic, Nonsulfhydryl Inhibitors of Ras Farnesylation. *Bioorg. Med. Chem.* **1997**, *5*, 93−99. (c) Njoroge, F. G.; Doll, R. J.; Vibulbhan, B.; Alvarez, C.; Bishop, W. R.; Petrin, J.; Kirschmeier, P.; Carruthers, N. I.; Wong, J. K.; Albanese, M. M.; Piwinski, J. J.; Catino, J.; Girijavallabhan, V.; Ganguly, A. K. Discovery of Novel Non-peptide Tricyclic Inhibitors of Ras Farnesyl Protein Transferase. *Bioorg. Med. Chem.* **1997**, *5*, 101−114. (d) Njoroge, F. G.; Vibulbhan, B.; Rane, D. F.; Bishop, W. R.; Petrin, J.; Patton, R.; Bryant, M. S.; Chen, K.-J.; Nomeir, A. A.; Lin, C.-C.; Liu, M.; King, I.; Chen, J.; Lee, S.; Yaremko, B.; Dell, J.; Lipari, P.; Malkowski, M.; Li, Z.; Catino, J.; Doll, R. J.; Girijavallabhan, V.; Ganguly, A. K. Structure−Activity Relationship of 3-Substituted *N*-Pyridinylacetyl-4-(8-chloro-5,6-dihydro-11H-benzo[5,6-]cyclohepta[1,2-b]pyridinyl-11-ylidene)piperidine Inhibitors of Farnesyl-Protein Transferase: Design and Synthesis of in Vivo Active Antitumor Compounds. *J. Med. Chem.* **1997**, *40*, 4290−4301.

(8) (a) Njoroge, F. G.; Taveras, A. G.; Kelly, J.; Remiszewski, S. W.; Mallams, A. K.; Wolin, R.; Afonso, A.; Cooper, A. B.; Rane, D.; Liu, Y.-T.; Wong, J.; Vibulbhan, B.; Pinto, P.; Deskus, J.; Alvarez, C.; Del Rosario, J.; Connolly, M.; Wang, J.; Desai, J. A.; Rossman, R. R.; Bishop, W. R.; Patton, R.; Wang, L.; Kirschmeier, P.; Bryant, M. S.; Nomeir, A. A.; Lin, C.-C.; Liu, M.; McPhail, A. T.; Doll, R. J.; Girijavallabhan, V.; Ganguly, A. K. (+)-4-[2-[4-(8-Chloro-3,10-dibromo-6,11-dihydro-5H-benzo[5,6]cyclohepta-[1,2-b]pyridin-11(*R*)-yl)-1-piperidinyl]-2-oxoethyl]-1-piperidinecarboxamide (Sch-66336): A Very Potent Farnesyl Protein Transferase Inhibitor as a Novel Antitumor Agent. *J. Med. Chem.* **1998**, *41*, 4890−4902. (b) Liu, M.; Bryant, M. S.; Chen, J.; Lee, S.; Yaremko, B.; Lipari, P.; Malkowski, M.; Ferrari, E.; Nielsen, L.; Prioloi, N.; Dell, J.; Sinha, D.; Syed, J.; Korfmacher, W. A.; Nomeir, A. A.; Lin, C.-C.; Wang, L.; Taveras, A. G.; Doll, R. J.; Njoroge, G.; Mallams, A. K.; Remiszewski, S.; Catino. J. J.; Girijavallabhan, V. M.; Kirschmeier, P.; Bishop, W. R. Antitumor Activity of Sch-66336, an Orally Bioavailable Tricyclic Inhibitor of Farnesyl Protein Transferase, in Human Tumor Xenograft Models and Wap-*ras* Transgenic Mice. *Cancer Res.* **1998**, *58*, 4947−4956.

(9) Strickland, C. L.; Weber, P. C.; Windsor, W. T.; Wu, Z.; Le, H. V.; Albanese, M. M.; Alvarez, C. S.; Cesarz, D.; del Rosario, J.; Deskus, J.; Mallams, A. K.; Njoroge, F. G.; Piwinski, J. J.; Remiszewski, S.; Rossman, R. R.; Taveras, A. G.; Vibulbhan, B.; Doll, R. J.; Girijavallbhan, V. M.; Ganguly, A. K. Tricyclic Farnesyl Protein Transferase Inhibitors: Crystallographic and Calorimetric Studies of Structure−Activity Relationships. *J. Med. Chem.* **1999**, *42*, 2125−2135.

(10) Bishop, W. R.; Doll, R. J.; Mallams, A. K.; Njoroge, F. G.; Petrin, J. M.; Piwinski, J. J.; Wolin, R. L.; Taveras, A. G.; Remiszewski, S. W. Tricyclic Amide and Urea Compounds, Useful Inhibition of G-Protein Function and for Treatment of Proliferative Diseases. U.S. Patent 5,807,853, September 15, 1998.

(11) Njoroge, F. G.; Taveras, A. G.; Doll, R. J.; Lalwani, T.; Alvarez, C.; Remiszewski, S. W. Compounds Useful for Inhibition of Farnesyl Protein Transferase. U.S. Patent 6,030,982, February 29, 2000.

(12) Njoroge, F. G.; Vibulbhan, B.; Bishop, W. R.; Kirschmeier, P.; Bryant, M. S.; Omeir, A. A.; Liu, M.; Doll, R. J.; Girijavallabhan, V. M.; Ganguly, A. K. Atropisomeric Trihalobenzocycloheptapyridine Analogues Provide Stereoselective FPT Inhibitors with Antitumor Activity. *Bioorg. Med. Chem.* **1999**, *7*, 861−867.

(13) Compound **22b** was prepared as described for **22a** in ref 10a and for **22c** in ref 8a.

(14) Benzocycloheptapyridine FTIs having C(11) *S* stereochemistry are reported to bind in reverse fashion relative to C(11) *R* enantiomers; see ref 9.

(15) Bryant, M. S.; Korfmacher, W. A.; Wang, S.; Nardo, C.; Nomeir, A. A.; Lin, C.-C. Pharmacokinetic Screening for Selection of New Drug Discovery Candidates is Greatly Enhanced Through the Use of Liquid Chromatography-Atmospheric Pressure Ionization Tandem Mass Spectrometry. *J. Chromatogr.* **1997**, *777*, 61−66.

(16) Dunitz, J. D. The Entropic Cost of Bound Water in Crystals and Biomolecules. *Science* **1994**, *264*, 670.

JM010463V